British Journal of Cancer

ARTICLE

Check for updates

Cellular and Molecular Biology

Thermal stress involved in TRPV2 promotes tumorigenesis through the pathways of HSP70/27 and PI3K/Akt/mTOR in esophageal squamous cell carcinoma

Rongqi Huang[1,2], Shuai Li[1,2], Chao Tian[3], Peng Zhou[4,5], Huifang Zhao[3], Wei Xie[4,6], Jie Xiao[4], Ling Wang[3], Jean de Dieu Habimana[1,2], Zuoxian Lin[1,7], Yuchen Yang[1,7], Na Cheng[1,7] and Zhiyuan Li[1,2,3,4,7,8]✉

BACKGROUND: The transient receptor potential vanilloid receptor 2 (TRPV2) has been found to participate in the pathogenesis of various types of cancers, however, its role(s) in the tumorigenesis of ESCC remain poorly understood.
METHODS: Western blotting and immunohistochemistry were performed to determine the expression profiles of TRPV2 in the ESCC patient tissues. A series of in vitro and in vivo experiments were conducted to reveal the role of TRPV2 in the tumorigenesis of ESCC.
RESULTS: Our study first uncovered that the activation of TRPV2 by recurrent acute thermal stress (54 °C) or O1821 (20 μM) promoted cancerous behaviours in ESCC cells. The pro-angiogenic capacity of the ESCC cells was found to be enhanced profoundly and both tumour formation and metastasis that originated from the cells were substantially promoted in nude mouse models upon the activation of TRPV2. These effects were inhibited significantly by tranilast (120 μM) and abolished by TRPV2 knockout. Conversely, overexpression of TRPV2 could switch the cells to tumorigenesis upon activation of TRPV2. Mechanistically, the driving role of TRPV2 in the progression of ESCC is mainly regulated by the HSP70/27 and PI3K/Akt/mTOR signalling pathways.
CONCLUSIONS: We revealed that TRPV2-PI3K/Akt/mTOR is a novel and promising target for the prevention and treatment of ESCC.

British Journal of Cancer (2022) 127:1424–1439; https://doi.org/10.1038/s41416-022-01896-2

INTRODUCTION

Malignant disease is a leading cause of human mortality. Esophageal cancer is the eighth most frequent cancer and the sixth most common cause of cancer death worldwide, accounting for over 5.4% of all cancer-related deaths [1, 2]. The incidence is 4.5 per 100,000 individuals in the USA, while some of the highest incidences are found in Southeastern Africa and the so-called Asian esophageal cancer belt (Turkey, Iran, Kazakhstan, and Northern and Central China) [3, 4], with approximately 100 per 100,000 individuals affected, more than 480,000 new cases diagnosed and 400,000 deaths yearly. Esophageal squamous cell cancer (ESCC) comprises the majority of esophageal malignancies (~90%), followed by adenocarcinomas [5]. In China, both the incidence and mortality of ESCC rank fourth among all cancers. ESCC remains one of the most lethal cancers among all malignancies, with a 5-year survival rate of <20% once diagnosed [6]. Reasons may be the lack of a sensitive method for early detection; thus, detectable regional and distant metastasis have occurred in most ESCC patients at the time of diagnosis [7, 8], and the limited clinical staging criteria lacks significant molecular biomarkers to effectively stratify patients for treatment options [9].

The pathogenesis of the disease has been suggested to be multifactorial, while the most important risk factors for ESCC are thought to be environmental, including tobacco smoking, alcohol drinking, dietary carcinogens (nitrosamines), insufficiency of micronutrients, exposure to polycyclic aromatic hydrocarbons (PAHs) and hot beverage consumption [10–13]. To cook foods on fire is one of mankind's first great innovations, however, consumption of beverages and food at high temperatures, which expose the esophageal mucosa to heat stimuli, has been documented to increase the risk of ESCC [14], and heat stimuli have been ranked as cause classification II for ESCC by the International Association of Cancer Registries (IACR) [15]. The pooled analysis adds evidence for a carcinogenic effect of chronic thermal injury in the oesophagus induced by the consumption of very hot drinks, including mate [16]. However, the underlying mechanism is poorly understood.

[1]CAS Key Laboratory of Regenerative Biology, Guangdong Provincial Key Laboratory of Stem Cell and Regenerative Medicine, Guangzhou Institutes of Biomedicine and Health, Chinese Academy of Sciences, Guangzhou, China. [2]University of Chinese Academy of Sciences, Beijing, China. [3]School of Life Sciences, University of Science and Technology of China, Hefei, China. [4]Department of Anatomy and Neurobiology, Xiangya School of Medicine, Central South University, Changsha, China. [5]Department of Pathology, the Second Xiangya Hospital of Central South University, Changsha, China. [6]Department of Hepatobiliary Surgery, Provincial Cancer Hospital of Hunan, Changsha, China. [7]Guangzhou Regenerative Medicine and Health Guangdong Laboratory, Guangzhou, China. [8]GZMU-GIBH Joint School of Life Sciences, Guangzhou Medical University, Guangzhou, China. ✉email: li_zhiyuan@gibh.ac.cn

Received: 11 March 2021 Revised: 28 May 2022 Accepted: 10 June 2022
Published online: 27 July 2022

The transient receptor potential vanilloid receptor 2 (TRPV2), one of the thermally sensitive TRP family members, has been reported to participate in the pathology of various types of human cancers, including prostate cancer [17], breast tumours [18], multiple myeloma [19] and hepatocellular carcinoma [20]. However, the role(s) of TRPV2 playing in the tumorigenesis of esophageal carcinoma, especially ESCC, remain largely unknown.

In this study, we found that the transient receptor potential vanilloid receptor 2 (TRPV2) was upregulated in ESCC cells compared to non-tumour esophageal squamous cells (NE2) and in clinical ESCC samples in comparison with adjacent non-tumour tissues. Furthermore, recurrent acute challenging of the cells with heat stimuli (54 °C, it is much lower than the dietary temperatures among many populations, but it could activate the TRPV2 channel in the cells) [21–23] significantly enhanced ESCC cancerous behaviours (proliferation, migration, invasion and angiogenesis) in vitro and markedly promoted tumorigenesis (tumour formation and metastasis) in vivo. The aggressiveness of ESCC cells was also augmented substantially upon the pharmaceutical activation of TRPV2. However, the tumorigenesis of ESCC was attenuated considerably by either inhibition of TRPV2 with tranilast (120 μM) (an antagonist of TRPV2) or TRPV2 knockout using CRISPR–Cas9. In contrast, overexpression of TRPV2 by transfection of a plasmid containing TRPV2 DNA into the non-tumour esophageal squamous cells (NE2), could switch the cells to tumorigenesis upon activation of TRPV2. Mechanistically, the role of TRPV2 in the progression of ESCC was found to be regulated by HSP70/27 and PI3K signalling pathways. Application of VS5584 (a pan-PI3K/mTOR kinase inhibitor) or oroxin B (a PTEN protein activator and PI3K/mTOR inhibitor) resulted in remarkably reduced proliferation of ESCC cells. Furthermore, the survival curve of ESCC patients showed that high expression level of TRPV2 was associated with a worse prognosis in ESCC patients. Together, our findings reveal a novel and important role of TRPV2 playing in the progression of ESCC upon thermal stress and identify the TRPV2-PI3K/Akt/mTOR pathway as a potential target for the prevention and treatment of ESCC.

MATERIALS AND METHODS

Plasmids and chemicals

pCMV6-TRPV2 and pCMV6-GFP were obtained from OriGene and maintained by our lab. Cas9-G418 plasmid was provided by Prof. Liangxue Lai of GIBH. O1821 and VS5584 were purchased from Cayman Chemical and MedChemExpress, respectively. Tranilast and oroxin B were both obtained from TargetMol, G418 was purchased for Merck. The chemicals were dissolved in DMSO (the maximal final concentration of DMSO was never exceeded 0.1% throughout the study) and diluted in PBS or extracellular solutions (pH 7.4) to obtain the desired concentrations. Agonists and antagonists were used at the concentrations based on our pre-experiments on ESCC cells and referred to the EC50 or IC50 as recommended by the suppliers. Matching volumes of DMSO were used as controls.

Cell culture

The human esophageal squamous cell carcinoma (ESCC) cell lines Eca-109 and TE-1 were obtained from the Cell Bank of the Chinese Academy of Sciences (Shanghai, China). Eca-109-gl (GFP and luciferase dually labelled Eca-109) cell line, Eca-109-VR2$^{-/-}$ (TRPV2 knocked-out Eca-109) cell line and Eca-109-VR2$^{-/-}$-gl (TRPV2 knocked-out and GFP− luciferase dually labelled Eca-109) cell line were established and maintained by our group. The ESCC cells were cultured in RPMI 1640 medium (Thermo Scientific, MA, USA) supplemented with 1 mM L-glutamine, and 10% (vol/vol) FBS. The immortalised normal esophageal squamous cell line NE2 (kindly provided by Prof. GSW Tsao, Hong Kong University), was cultured in a 1:1 ratio of defined keratinocyte-SFM (DKSFM) supplemented with growth factors (Thermo Scientific, MA, USA) and Epi-life medium supplemented with Epi-life Defined Growth Supplement (EDGS) growth factors (Thermo Scientific, MA, USA). HUVECs were obtained from American Type Culture Collection and were maintained in DMEM (Thermo Scientific, MA, USA) supplemented with 10% (vol/vol) FBS. Cell lines were authenticated using short tandem repeat profiling by the direct suppliers or by our institute (HUVECs). Routine *Mycoplasma* testing was performed by MycoAlert Mycoplasma Detection Kit (#LT07-318, Lonza) every 3–6 months. Cells were cultured in a humidified incubator with 5% CO_2 at 37 °C. Unless otherwise indicated, the medium was replaced every 3 days, and the cells were subcultured when they reached 85% confluence.

Soft-agar assay

Anchorage-independent growth was determined by a soft-agar clonogenesis assay. Five thousand ESCC cells and 1×10^4 NE2 cells were suspended in 0.75 ml of RPMI 1640 growth medium (Thermo Scientific, MA, USA) or 0.75 ml of defined keratinocyte-SFM (DKSFM) plus Epi-life medium (Thermo Scientific, MA, USA) and mixed with 0.75 ml of 0.66% agarose (BioWest, Nuaillé, France), respectively, then the mixtures were immediately layered onto six-well plates precast by mixing 0.75 ml of 1% agarose (BioWest, Nuaillé, France) with 0.75 ml of RPMI 1640 medium or 0.75 ml of Defined Keratinocyte-SFM (DKSFM) plus Epi-life medium (Thermo Scientific, MA, USA). The cells were allowed for consecutive culture up to 2 weeks. The medium of the top layer was replaced every week. The colonies with more than 50 cells were captured under an inverted microscope.

Intracellular calcium imaging

Cells were cultured in 3 cm-diameter glass-bottom dishes for 24 h, thereafter medium was discarded and dishes were washed using 4 °C Hank's balanced salt solution (HBSS, Genom Biotech, Hangzhou, Zhejiang, China), then cells were pre-incubated with 5 μM Fura-2–AM (Dojindo Laboratories) in 1 ml HBSS in the dishes for 45 min at 37 °C in the dark. Subsequently, the pre-incubated solution was pipetted away and cells were washed three times with HBSS to eliminate the extracellular Fura-2AM, then 1 ml of HBSS was added and cells were incubated at 37 °C in the dark for 20 min for the full de-esterification of intracellular Fura-2AM. The dishes were mounted on the stage of an inverted microscope (Eclipse Ti-U, Nikon, Tokyo, Japan). Unless indicated otherwise, Fura-2AM fluorescence was measured at room temperature (24–25 °C) using a digital imaging system (MetaFluor software, Molecular Devices, CA, USA) and alternately exposed to excitation wavelengths of 340 and 380 nm. The field of interest contained 20–40 fluorescent cells. Results were plotted as a mean ratio of F340/380 nm ± SEM, and *n* values indicate the number of experiments per data point. The measurements lasted between 3.5 and 6.5 min. During the first min, $[Ca^{2+}]_i$ baseline levels were measured. A control test using the control dish was run through the equal time course of each Ca^{2+} imaging measurement. Some TRPV channel activators and inhibitors were dissolved in a stock solvent dimethyl sulfoxide (DMSO) and further diluted in HBSS to obtain the desired working solutions. The DMSO concentration did not exceed 0.1% which would not affect $[Ca^{2+}]_i$ (data not shown). Drug administration and washout were conducted manually during the experiments. For thermal stimulation, HBSS was heated via a water bath in Eppendorf tubes in a mini thermostat (TZ, Suzhou, Jiangsu, China) to the desired temperature and the heated HBSS was applied to cells manually, and then, the HBSS temperature was monitored by an infrared thermometer (Wahome, Zhongshan, Guangdong, China).

Drug administration and thermal stimulation protocol

Cells were pretreated with the indicated dose of TRPV2 activator and/or inhibitor (dissolved and remained in culture medium until next medium renewal, medium was replaced twice per day) or exposed to heat (54 °C) stimulation (water bath, thrice per day, 30 s per time) or heat (54 °C) stimulation and/or tranilast (120 μM), VS5584 (95 nM) or oroxin B (156 nM), respectively, for up to 14 days. Heat stimulation was performed as described previously [24]. Briefly, cells cultured in six-well plates were exposed to heat stimulation in a water bath thermostat. The water bath temperature (T) was set to 5–7 °C higher than each T_{tested} for quick thermal conduction through the base of the culture plate. The water bath temperature was automatically maintained by a thermostat. A plastic holder that fits a six-well plate was placed into the water in the thermostat, then the medium was pipetted away, and the plates were positioned on the holder and immersed ~6 mm depth in the water. Temperatures of the inner surface of the plates were monitored by an infrared thermometer. Cells were exposed to corresponding drugs or heat stimuli for the indicated time course. Agonists and antagonists were used at the concentrations based on our pre-experiments on ESCC cells and referred

to the EC50 or IC50 as recommended by the suppliers. The frequency and duration of heat stimulations were based on our pre-experiments on the same cell lines. Matching volumes of DMSO were used as controls.

Protein extraction and western blotting

Protein extraction from cell lines and patient tissues and western blotting was performed as previously described [24, 25]. Briefly, cells or tissues were washed by cold PBS on ice, and then, cells were lysed with a buffer containing Tris/HCl (50 mM), NaCl (150 mM), NaN_3 (0.02%), Nonidet P-40 (1%), SDS (0.1%), sodium deoxycholate (0.5%), leupeptin (0.5 mg mL^{-1}), 500 μM phenylmethylsulfonyl fluoride, and aprotinin (1 μg mL^{-1}). The cell lysate was centrifuged at 13,000 × *g* for 20 min at 4 °C. After this, the supernatant was carefully collected for western blotting. Protein concentration was determined with BCA kit (Genstar, Beijing, China). The proteins were separated by SDS/PAGE and transferred to nitrocellulose membranes (Pierce, Waltham, Massachusetts, USA), which were blocked at room temperature (24–26 °C) for 1 h in 5% nonfat milk solution. The membranes were incubated at 4 °C overnight with primary antibodies, including rabbit anti-human TRPV2 (#sc-30155, Santa Cruz), rabbit anti-human β-actin (#5125, CST), rabbit anti-human HIF1 (#A11945, Abclonal), rabbit anti-human TNFα (#A0277, Abclonal), rabbit anti-human NFkB (#A11163, Abclonal), rabbit anti-human HSP27 (#A0240, Abclonal), rabbit anti- human HSP40 (#A5504, Abclonal), rabbit anti-human HSP60 (#A0969, Abclonal), rabbit anti-human HSP70 (#A0284, Abclonal), rabbit anti-human HSP90 (#A1087, Abclonal), rabbit anti-human Calmodulin (#abs133163, Absin), rabbit anti-human PTEN (#abs134055, Absin), rabbit anti-human AKT1 (#sc-5298, Santa Cruz), rabbit anti-human PI3K (#A0265, Abclonal), rabbit anti-human PDK1 (#abs131621, Absin), rabbit anti- human mTORC1 (#sc-517464, Santa Cruz), rabbit anti-human p-mTOR (Ser2448) (#5536S);rabbit anti-human p-p70S6K (Thr389) (#9234S); rabbit anti-human p-4EBP1 (Ser65) (#13443S); rabbit anti-human p-Akt (Thr308) (#13038S); rabbit anti-human p-Akt (Ser473) (#4060S), respectively. Horseradish peroxidase-linked secondary antibodies (goat anti-rabbit IgG, Beyontime, Nanjing, Jiangsu, China) were used. Final detection was accomplished with western blot luminol reagents (Thermo Scientific, Waltham, MA, USA). Densitometric quantification of corresponding protein bands was carried out by using ImageJ software (Bethesda, MD, USA).

Real-time qPCR analysis

Total RNA from Eca-109 cells following the treatment as described in "Drug administration and thermal stimulation protocol" was isolated using TRIzol Reagent (Tiangen, Beijing, China) according to the manufacturer's instructions. The concentration of RNA was measured by the NanoDrop 2000 Spectrophotometer (Thermo Fisher Scientific, Rockford, IL, USA). The first-strand cDNA was synthesised from 1 μg of total RNA using HiScript® III RT SuperMix (Vazyme, Nanjing, China). The quantitative PCR experiments were performed on a CFX96 Touch™ Real-Time PCR system (Bio-Rad) using Taq Pro Universal SYBR qPCR Master Mix (Vazyme, Nanjing, China) with gene-specific primers. Beta-actin (β-actin) was used as an internal control for normalisation. Primer sequences used in this study are listed in Supplementary Table S1. All reactions were conducted in triplicate, and the relative expression of mRNA levels was calculated using the $2^{-\triangle\triangle Ct}$ method.

Immunofluorescence analysis and microscopy

For immunocytochemical analysis, cells were seeded on coverslips in a large Petri dish overnight for cell attachment, and then, the coverslips were washed with cold PBS 3 min each time for three times to discard the debris of cells and medium, and the cells were fixed on the coverslips with 4% paraformaldehyde for 15 min. After fixation, the cells were washed by PBS 3 min each time for three times and were permeabilized with 0.1% Triton X-100 in PBS for 20 min; thereafter, cells were washed by PBS 3 min each time for three times. Subsequently, the cells were blocked with 3% BSA for 1 h at room temperature. Rabbit anti-human TRPV2 primary antibody (#sc-30155, Santa Cruz) and Alexa Fluor 594 goat anti-rabbit secondary antibody (#ab-150080, Abcam) were used according to the manufacturers' instructions. The primary antibody was incubated overnight at 4 °C and then washed 3 min each time for three times in PBST (PBS supplemented with 0.1% Tween-20). The cells were incubated with the secondary antibody (1:1000 dilution in 3% BSA) at room temperature for 1 h and then washed 3 min each time for three times with PBST. All cells were incubated with DAPI for 6 min to stain the nucleus then washed 3 min each time for three times by PBST. Each coverslip was mounted onto 10 μL of antifading solution on a glass slide. All images were taken on a confocal laser scanning microscope (LSM-710, Zeiss) and analysed with the ZEISS LSM (Oberkochen, Germany) image examiner software and Adobe Photoshop.

Plasmid DNA transfection

An NE2 cell suspension of 2.5×10^6 cells/ml in electroporation buffer was mixed with a 3 μg/μl pCMV6-TRPV2 and pCMV6-GFP solution at a 4:1 ratio to a final concentration of 0.6 μg/μl for each pDNA. Then the mixture was transferred into a cuvette. Transfection was achieved by electroporation with the Neon™ transfection system (Life technology) at 1350 V, 30 ms, 1 pulse. Subsequently, the cells were immediately transferred into the wells of a six-well culture plate containing 2 ml of medium/well to ensure proper cell recovery. The plate was incubated at 37 °C in 5% CO_2 for further experiments.

gRNA and CRISPR/Cas9 vector protocols

The protocols for sgRNA design, vector construction and in vitro transcription were conducted according to previously published protocols [26]. First, the sgRNAs targeting the human TRPV2 gene (NC_000017.11) were designed using the online CRISPR Design Tool (http://crispr.mit.edu/). Then, the complementary oligo sgRNAs were cloned into the BbsI sites of a Puc57-T7-sgRNA cloning vector (Addgene ID51306). The amplified PCR products of the Puc57-T7-sgRNA vector were transcribed in vitro using the MAXIscript T7 Kit (Ambion) and purified with the miRNeasy Mini Kit (Qiagen) according to the manufacturers' instructions. Finally, 1×10^6 Eca-109 cells were transfected with 4 μg Cas9-G418 plasmid and 1 μg of each TRPV2 sgRNA plasmid by nucleoporation (Lonza). The transfected cells were divided into twenty 10-cm culture dishes and recovered for 24 h. After cell recovery, 1 mg/mL G418 (Merck) was added to the culture medium. After 8–12 days of selection, G418-resistant colonies were picked and cultured in 24-well plates by using cloning cylinders. Upon 70–80% confluence, the cell colonies were subcultured, and 10% of each colony was lysed individually in 10 μL of NP-40 lysis buffer (0.45% NP-40 plus 0.6% Proteinase K) for 60 min at 56 °C and then for 10 min at 95 °C. The lysate was used as a template for PCR screening, which was performed using Long PCR Enzyme Mix (Thermo Scientific, Waltham, MA, USA), in accordance with the manufacturer's instructions. The positive cell colonies were expanded and six colonies were cryopreserved in liquid nitrogen for further experiments.

Off-target analysis

The POT sites for each sgRNA were predicted to analyse site-specific edits by the BE3 system according to an online design tool (http://www.rgenome.net/cas-offinder/) [27]. All POTs were amplified by PCR and then subjected to Sanger sequencing to confirm the off-target effects, respectively. The primers for amplifying the off-target sites are listed in Supplementary Table S1.

Cell proliferation assay

Cell proliferation was evaluated via a single-cell culture assay. Cells following treatment as described in "Drug administration and thermal stimulation protocol" were trypsinized, then suspended and diluted to a concentration of one cell per 10 μl. Subsequently, 10 μl of each cell suspension was seeded per well in a 48-well culture plate. The seeded cells were observed under an inverted microscope (Nikon) and wells with more than one cells were excluded from the assay. The cell numbers were counted manually under the inverted microscope or by imaging all the cell clones and further processed via ImageJ software (Bethesda, MD, USA).

Cell wound-healing assay

Four parallel lines were drawn on the back of the six-well plates with a marker pen before cell seeding. Cells following the treatment as described in "Drug administration and thermal stimulation protocol" were applied to seeding on the six-well plates. On the following day, the culture medium was removed and replaced with 0.5% FBS/RPMI 1640 medium. Twenty-four hours later, a straight wound line that was perpendicular to those parallel lines was drawn across the attached and almost 100% confluent cell layer with yellow pipette tips. Therefore, the wound gap between two parallel lines was marked. Pictures of the marked gap were taken at 24 h and 48 h after the gaps were created. The wound gaps (in mm) were quantified by using IMAGE-PRO PLUS software and calculated by the

equation: % migration distance = ($gap_{0\ h\ treated}$——$gap_{24\ h}$ or $_{48\ h\ treated}$)/($gap_{0\ h\ control}$——$gap_{24\ h}$ or $_{48\ h\ control}$) *100%.

Three-dimensional invasion assay

AIM chips (AIM Biotech, Singapore) were assembled according to the manufacturer's instructions. Matrigel (#354248, Corning) was used to fill the gel tunnel from one side all the way to the other side. The gel-filled chips (on AIM holders) were placed into a 37 °C incubator and incubated for 30 min to allow the polymerisation of Matrigel. Cells following the treatment as described in "Drug administration and thermal stimulation protocol" were trypsinized and diluted to a density of 1×10^6. A micropipette was used to withdraw 10 µl of cell suspension. The tip was directed near the inlet of the medium channel and the cell suspension was injected. After 2 min, the same procedure was repeated for the opposite connecting inlet. In total, 20 µl of cell suspension was seeded per medium channel. To exchange medium in a medium channel, 70 µl of medium was added into one port and then 50 µl was added to the opposite connecting port. Cells were filled and allowed to invade the gel tunnel and were visually inspected under an inverted microscope (Nikon); invaded cells were manually counted in ten fields and compared. The furthest distances of the invaded cells (away from the starting point) were measured and compared.

Tube-formation assay

Eca-109 and Eca-109-TRPV2$^{-/-}$ cells followed the indicated treatment as described in "Drug administration and thermal stimulation protocol" were cultured in 6-well plates with 2 ml fresh serum-free medium for 24 h, then the 24 h′ conditioned medium was collected for tube-formation assay. A 48-well plate was pre-coated with 125 µl Matrigel (#354248, Corning) and allowed to solidify at 37 °C for 1 h. Then HUVECs (1×10^5) resuspended with the conditioned medium were layered onto the Matrigel and monitored over time for the formation of tube-like structures. Endothelial cell formation was observed, and photos were captured 48 h later under an inverted microscope (Nikon). Relative quantities of the tubules were quantified by ImageJ software (Bethesda, MD, USA).

ELISA analysis

Eca-109 cells following treatment as described in "Drug administration and thermal stimulation protocol" were cultured at a density of 1×10^5 cells/well in six-well plates for 24 h. Thereafter, cells were washed three times using PBS and changed to fresh serum-free medium for an additional 24 h. Then the supernatants were harvested, centrifuged at 3600 rpm for 5 min, and used as conditioned medium (CM). Secretion of vascular endothelial growth factor (VEGF), the main pro-angiogenic factor, in CM was determined using human VEGF ELISA kits (ExCell, Shanghai, China) according to the manufacturer's instructions. Absorbance at 450 nm was recorded with a SpectraMax microplate reader.

In vivo tumorigenicity and metastasis assay

Male BALB/c nude mice (3–4 weeks of age, 18–20 g) were purchased from Vital River Laboratories (Beijing, China). All of the animal studies were conducted under protocols approved by the guidelines of the Ethics Committee of Animal Experiments at GIBH. All animal work was conducted in the Laboratory Animal Center, GIBH. The BALB/c nude mice were randomly divided into 6 groups ($n = 4$–7 mice/group). Five million Eca-09 cells following the treatment as described in "Drug administration and thermal stimulation protocol" were mixed at a ratio of 1:1 (v/v) with Matrigel (#354248, Corning) and injected subcutaneously into the left flank of 4- to 5-week-old male BALB/c nude mice. Tumour volumes were determined every 3 days, and were calculated using the equation $0.52 \times a \times b^2$, where a and b are the largest and smallest lengths of the tumour, respectively. GFP and luciferase (GL)-expressing tumour cells (Eca-109-gl or Eca-109-VR2$^{-/-}$-gl, 1×10^5) were i.v. through the tail vein into BALB/c nude mice to establish metastatic models. To generate bioluminescence signals, D-luciferin (3 mg/100 µl per mouse, Yeasen Biotech, Shanghai, China) was injected i.p. 5 min before the image acquisition. Mice were anaesthetised with 1.5% isoflurane and image data were acquired by 15 s exposure using the IVIS Spectrum at an interval of 2 weeks and analysed using the Living Image software (PerkinElmer). On day 45 or 49, animals were euthanized by full CO_2 inhalation, and tumours were excised, weighed, photographed and lungs were paraffin-embedded for further experiments.

IHC, and hematoxylin and eosin (H&E) staining of mouse tissues

Serial 4.0-µm lung sections were cut and subjected to IHC staining using an anti-Ki-67 (#abs131599, Absin, Shanghai, China) and anti-CD31 antibody ((#abs131735, Absin, Shanghai, China) or H&E stained with Mayer's hematoxylin solution. IHC and H&E staining were performed according to standard protocols. The images were captured using the Computerised Image Analysis System (Carl Zeiss). The microvessel density (MVD) was quantified by counting the proportion of CD31-positive cells. The proliferation index was quantified by counting the proportion of Ki-67-positive cells.

Fresh clinical tissue specimen collection and processing

Fresh human esophageal squamous tumours and adjacent non-tumour tissue specimens were obtained from 35 patients undergoing esophageal resection for ESCC (four patients with poor sample quality were later excluded from the trial). For the use of these clinical materials for research purposes, prior patient consent and approval from the Institutional Research Ethics Committee were obtained. Specimens were collected between 2017 and 2018 at the Cancer Hospital of Hunan Province in Changsha, China. Samples were transferred to our lab via cold-chain transportation and prepared for further experiments. The clinical information of the patients is summarised in Supplementary Table S2.

Human esophageal cancer tissue specimens and IHC

We obtained paraffin-embedded tissue samples in accordance with the ethical standards of the Institutional Committees on Human Experimentation from 193 consecutive patients with esophageal squamous cell carcinoma who had undergone surgery without preoperative chemotherapy or radiotherapy between 2012 and 2013 at the Second Affiliated Hospital of Xiangya Medical School of Central South University, Changsha, China. Corresponding specimens from each patient's distant (5 cm from the tumour lesions) normal tissue were also collected in each case. Serial 3.0–4.0-µm sections were cut and subjected to IHC staining using an anti-TRPV2 antibody (#sc-30155, Santa Cruz). IHC staining was performed according to standard protocols. The clinical information of the patients is summarised in Supplementary Table S2.

Kaplan–Meier and multivariate analysis

The relationship between the expression of TRPV2 and the prognosis of ESCC patients was investigated using data provided by authors of previous publications [28, 29]. Disease-specific survival (DSS) was calculated from the time of surgery to the time of death from ESCC. Disease-free survival (DFS) was calculated from the time from surgery to the first recurrence of index cancer or to all-cause death. To the time of last follow-up or death from disease other than ESCC, at which point, the data were censored. Survival curves were calculated by the Kaplan–Meier method and analysed by log-rank test. To determine independent factors that were significantly related to the prognosis, multivariate analysis was performed using Cox's proportional hazards regression model with a forward stepwise procedure. All eligible patients provided written informed consent. Patient information and pathological characteristics are shown in Supplementary Table S3.

Statistical analysis

Results are presented as mean ± SD. Data were analysed by one-way ANOVA or two-way ANOVA followed by Bonferroni's post hoc test unless otherwise stated. All data and statistical analyses were performed by Origin 9.1 or GraphPad Prism 8 software. $P < 0.05$ was considered statistically significant. Asterisks indicate statistical difference as follows: ns, not significant; *$P < 0.05$; **$P < 0.01$; ***$P < 0.001$.

RESULTS

TRPV2 is upregulated in ESCC cells, and overactivation of TRPV2 promotes cell proliferation

Transient receptor potential vanilloid receptor 2 (TRPV2) is functionally thermosensitive and can be activated by heat at high temperature (>52 °C) [30]. To explore the expression of TRPV2 in ESCC cells (Eca-109 and TE-1) and non-tumour esophageal squamous cells (NE2) (the anchorage-independent growth of the cell lines was tested by a soft-agar colony formation assay,

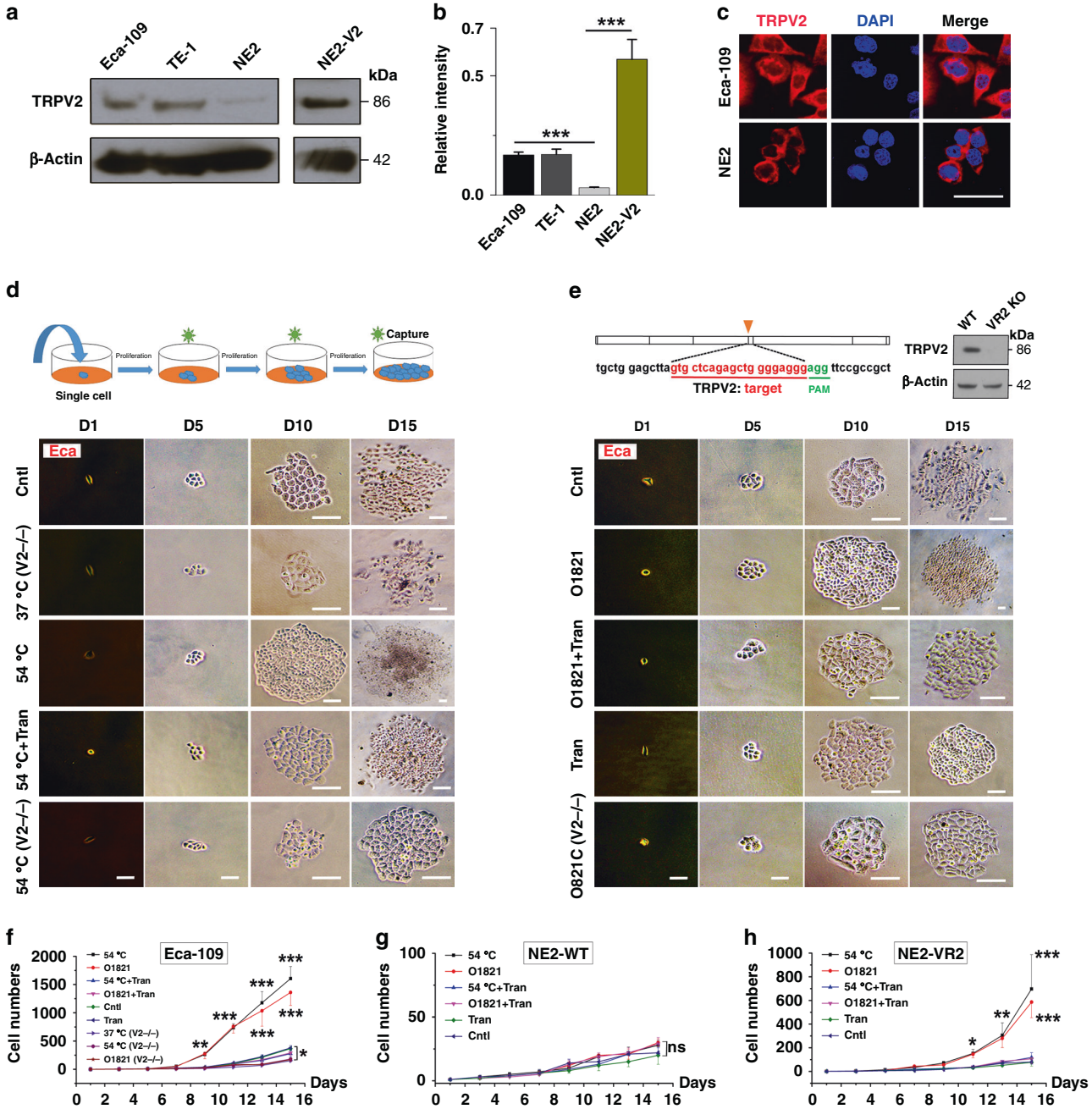

Fig. 1 TRPV2 is upregulated in ESCC cells, and overactivation of TRPV2 promotes cellular proliferation. a Western blotting showing the expression pattern of TRPV2 (86 kDa) among ESCC cells (Eca-109 and TE-1) and non-tumour cells (NE2). Ectopic expression of TRPV2 in the NE2 cells was as control and β-actin (42 kDa) was used as an internal control. **b** Densitometric quantification of TRPV2 protein among the three cell lines ($n = 6$). **c** ICF staining showing the expression of TRPV2 in Eca-109 and NE2 cells (TRPV2 in red) ($n = 5$). **d** Upper: outline of the single-cell culture assay for cellular proliferation. Lower: representative images of Eca-109 or TRPV2 knocked-out Eca-109 ($V2^{-/-}$) cells in the single-cell proliferation assay. Cultured Eca-109 cells without specific treatment were used as controls. Images were serially captured at 4-day intervals. **e** Upper: the targeted segment of the TRPV2 gene for CRISPR–Cas9 editing and western blotting showing that the knockout cells are devoid of TRPV2 protein ($n = 3$). Lower: representative images of Eca-109 or TRPV2 knocked-out Eca-109 ($V2^{-/-}$) cells in the single-cell proliferation assay. **f** Eca-109 or TRPV2-knockout Eca-109 ($V2^{-/-}$) cell numbers were relative to the control cell numbers and plotted over a time course ($n = 20–30$). **g** Wild-type (WT) NE2 cell numbers were relative to the control cell numbers and plotted over a time course ($n = 20–30$). **h** Cell numbers of NE2 with ectopically expressed TRPV2 (VR2) were relative to the control cell numbers and plotted over a time course ($n = 20–30$). Eca Eca-109, Cntl control, Tran tranilast. Scale bar: 10 μm. $^*P < 0.05$, $^{**}P < 0.01$, $^{***}P < 0.001$ by Student *t* tests for western blotting and two-way ANOVA tests for proliferation assay.

Supplementary Fig. S1A), RT-qPCR and western blot were carried out. TRPV2 mRNA and protein (86 kDa) were detectable among all three cell lines, and the expression of TRPV2 was found to be upregulated in ESCC cells at both transcriptional and translational levels compared with NE2 cells (Fig. 1a, b and Supplementary Fig. S1C). To further examine the expression and localisation of TRPV2 among these cell lines, immunocytofluorescence was carried out. TRPV2 was found to be expressed and localised predominantly in the plasma membrane of ESCC cells and NE2 cells (Fig. 1c and Supplementary Fig. S1B).

Cellular proliferation viability was evaluated via a single-cell culturing assay, based on previous studies that tumours could originate from a single cell and further grow uncontrollably, eventually leading to a malignant state [31, 32] and our observation that tumour cells are more tolerant of "unfavourable" conditions than non-tumour cells, therefore they could survive an extremely scarce nutritious environment.

Cellular proliferation of Eca-109 was promoted significantly upon exposure to recurrent brief heat stimuli (54 °C) or frequent application of O1821 (20 μM). The TRPV2 agonist O1821 is a synthetic cannabinoid that stimulates TRPV2, but does not stimulate TRPV1 or the cannabinoid receptors [33, 34], which could activate TRPV2, as confirmed by a calcium-imaging assay (Supplementary Fig. S2A–L). In this study, the term "overactivation" was used to describe the abovementioned patterns of heat treatment (54 °C) or the application of O1821 (20 μM), which could cause frequent activations of TRPV2. The pro-proliferative effects on Eca-109 cells were abrogated by either simultaneous application of tranilast (120 μM), a TRPV2 antagonist, or by TRPV2 knockout using CRISPR–Cas9 (Fig. 1d–f). Similar effects could be observed in another ESCC cell line, TE-1 (Supplementary Fig. S3A, B). It is worth noting that cellular proliferation of Eca-109, either under normal culturing conditions or after exposure to heat treatment (54 °C) or the application of O1821 (20 μM), was decreased substantially by the knockout of TRPV2 (Fig. 1d–f). The proliferation of wild-type NE2 (NE2-WT, which was with a low expression level of TRPV2, Fig. 1a, b) cells was affected by neither exposure to recurrent brief heat stimuli (54 °C) nor the application of O1821 (20 μM) (Fig. 1g and Supplementary Fig. S3C).

Conversely, when the proliferation assay was conducted on NE2 cells with ectopically expressed TRPV2 (NE2-VR2), the cellular proliferation of NE2 cells was enhanced markedly upon exposure to recurrent brief heat stimuli (54 °C) or O1821 (20 μM), and these effects were attenuated by tranilast (120 μM) (Fig. 1h and Supplementary Fig. S3D). Notably, even under normal culturing conditions, the cellular proliferation of NE2 cells with ectopically expressed TRPV2 appeared to be significantly greater than that of wild-type NE2 cells. Together, these data indicated that overexpression and overactivation of TRPV2 could promote the proliferation of esophageal squamous cells and upregulation of TRPV2 might play a role in the pathology of ESCC.

Overactivation of TRPV2 enhances the migration and invasion of ESCC cells in vitro

To assess the impact of TRPV2 activation on ESCC cell migration, a wound-healing assay was applied. Cellular migration of ESCC cells (Eca-109 and TE-1) was considerably accelerated upon the activation of TRPV2 by recurrent brief heat (54 °C) stimuli or administration of O1821 (20 μM), and these effects were abolished by either the TRPV2 antagonist, tranilast (120 μM), or by TRPV2 knockout using CRISPR–Cas9 (Fig. 2a, b and Supplementary Fig. S4A, B). These data suggested that overactivation of TRPV2 could promote the migratory ability of ESCC cells. On the other hand, the migratory ability of wild-type NE2 cells (NE2-WT, which had a low expression level of TRPV2, Fig. 1a, b) remained unaffected upon the overactivation of TRPV2 by heat (54 °C) stimuli or O1821 (20 μM) treatment (Fig. 2c and Supplementary Fig. S4C). Conversely, cellular migration was enhanced profoundly upon the overactivation of TRPV2 by both cues in the NE2 cells with ectopically overexpressed TRPV2 (NE2-VR2) (Fig. 2d and Supplementary Fig. S4D), hence further verifying the promigratory role of TRPV2 in the cells.

To evaluate the cellular invasive process, we used a new platform adopting AIM 3D chips [35]. The trajectory of invasive cells can be monitored over time during the experiments, and the invasive process (including invasive cell numbers and furthest invaded distance by the frontmost cell) can be easily visualised and measured using these chips in the assay, compared with the traditional way of using Boyden chambers [36–38]. The number of invasive ESCC cells (Eca-109 and TE-1) and the furthest invaded distance of these cells were enhanced markedly by recurrent brief heat (54 °C) stimuli or exposure to O1821 (20 μM), and these effects were attenuated significantly by tranilast (120 μM) or by TRPV2 knockout using CRISPR–Cas9 (Fig. 2e, f and Supplementary Fig. S5A–C). It is noteworthy that both cellular migration and invasion of Eca-109 cells was significantly inhibited by the knockout of TRPV2 ((Fig. 2a, b, e, f and Supplementary Fig. S5A, C). Taken together, these findings suggested that overactivation of TRPV2 could promote the migratory and invasive ability of ESCC cells.

For the non-tumour line, the invasive ability (including invasive cell numbers and furthest invaded distance) of wild-type NE2 (NE2-WT) cells were affected neither by the overactivation of TRPV2 by recurrent brief heat stimuli (54 °C) nor by O1821 (20 μM) treatment, whereas the invasive ability (including invasive cell numbers and furthest invaded distance) of ectopically expressed TRPV2 NE2 (NE2-VR2) cells was elevated substantially upon the overactivation of TRPV2 by recurrent brief heat stimuli (54 °C) or O1821 (20 μM) administration. Again, these effects were abolished by tranilast (120 μM) (Fig. 2g and Supplementary Fig. S5C), which further corroborates the pro-invasive role of TRPV2.

Overactivation of TRPV2 in ESCC cells promotes tumour-related angiogenesis

The capability to promote angiogenesis within or surrounding the tumour tissue is a hallmark of many oncogenic factors [39]. To examine the impact of TRPV2 overactivation in ESCC cells on angiogenesis, a tube-formation assay was applied (Fig. 3a). Human umbilical vein endothelial cells (HUVECs) were used as angiogenesis progenitor cells. The recruitment of HUVECs and the total length of newly formed microvessels were all significantly promoted by conditioned medium derived from Eca-109 cells following the overactivation of TRPV2 by recurrent brief heat stimuli (54 °C) or the treatment with O1821 (20 μM), and these effects were attenuated remarkably by tranilast (120 μM). Meanwhile, the pro-angiogenic effect (on the total length of newly formed microvessels) of the conditioned medium derived from Eca-109-VR2$^{-/-}$ (TRPV2 knocked-out Eca-109) cells following recurrent brief heat stimuli (54 °C) was arrested (Fig. 3b, c). Furthermore, the number of junctions and branches of the newly formed microvessels was also significantly increased by the conditioned medium derived from Eca-109 cells following the overactivation of TRPV2 by recurrent brief heat stimuli (54 °C) or by the administration of O1821 (20 μM), and these effects were markedly inhibited by tranilast (120 μM). Conditioned medium derived from Eca-109-VR2$^{-/-}$ cells following recurrent brief heat stimuli (54 °C) induced much less microvessel formation (with much fewer junctions and branches of the newly formed microvessels) versus the control in the assay (Fig. 3b, d, e).

To further explore the angiogenesis-promoting effect of overactivation of TRPV2, the levels of VEGF, the main pro-angiogenic factor, were measured in the corresponding conditioned medium by ELISA. In line with the tube-formation results (Fig. 3b–e), the levels of VEGF were much higher in the conditioned medium derived from Eca-109 cells following the overactivation of TRPV2 by recurrent brief heat stimuli (54 °C) or the treatment with O1821 (20 μM) when compared with those of groups simultaneously treated with tranilast (120 μM), indicating that overactivation of TRPV2 promoted VEGF secretion from the ESCC cells. Moreover, conditioned medium derived from Eca-109-VR2$^{-/-}$ cells following recurrent brief heat stimuli (54 °C) contained significantly less VEGF, suggesting that the knockout of TRPV2 could inhibit the secretion of VEGF from the ESCC cells (Fig. 3f). The secretions of VEGF underlie the microvessel morphogenesis that mutually corroborate the microvessel phenotype. Collectively, these findings indicated that overactivation of TRPV2 could promote

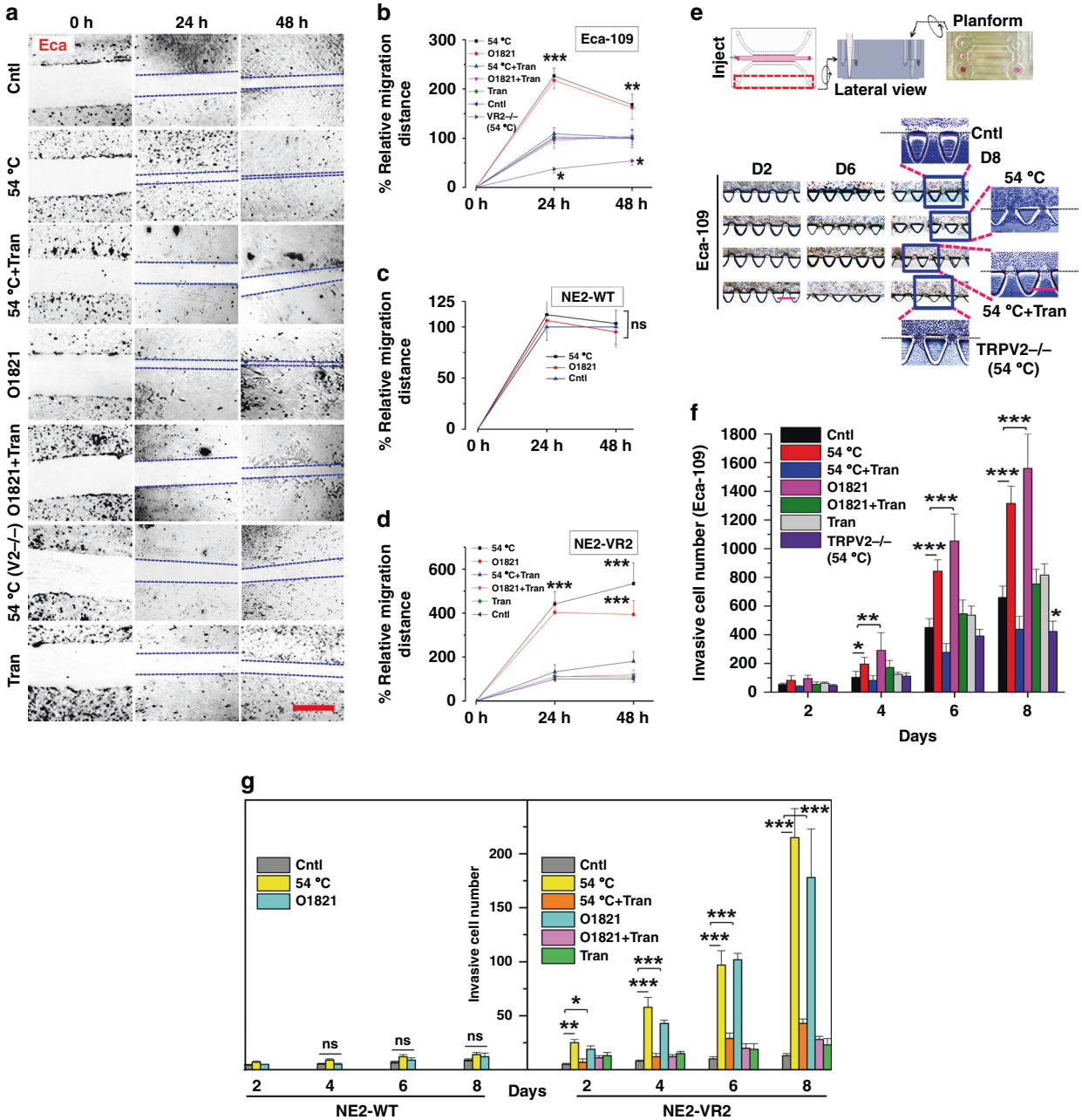

Fig. 2 Overactivation of TRPV2 promotes the migration and invasion of ESCC and ectopically expressed TRPV2 NE2 cells. **a** Representative images of Eca-109 cell migration in the wound-healing assay. Cultured Eca-109 cells without specific treatment were used as controls. **b** Cellular migration of Eca-109 was promoted substantially by exposure to heat stimuli (54 °C) or O1821 (20 μM); these effects could be abrogated by tranilast (120 μM) or by knockout of TRPV2 using CRISPR–Cas9 ($n = 4$). **c** Wild-type NE2 cell migration was affected neither by exposure to heat stimuli (54 °C) nor by application of O1821 (20 μM) ($n = 3$). **d** Migration of NE2 cells with ectopically expressed TRPV2 was enhanced markedly by exposure to heat stimuli (54 °C) or O1821 (20 μM), and these effects were abrogated by tranilast (120 μM) ($n = 3$). **e** Upper: schematic diagram of the 3D culturing assay for cellular invasion. Lower: sample images of Eca-109 cells invading the Matrigel in the 3D-culture assay. Invaded cells (beneath the dotted line) were manually counted in ten fields of each chip. Cultured Eca-109 cells without specific treatment were used as controls. **f** Invasive cells (Eca-109) were counted under a microscope, and the count were averaged, plotted against a time course ($n = 4$). **g** Invasive cells of wild-type NE2 (WT) and NE2 with ectopically expressed TRPV2 (VR2) were counted under a microscope, and the count were averaged, plotted against a time course ($n = 3$). Eca Eca-109, Cntl control, Tran tranilast, $TRPV2^{-/-}$ (or $V2^{-/-}$) TRPV2-knockout Eca-109 cell line. Scale bar: 1.0 mm. $^{*}P < 0.05$, $^{**}P < 0.01$, $^{***}P < 0.001$ by two-way ANOVA tests.

tumour-related angiogenesis in ESCC cells and thus might promote the tumorigenesis of ESCC.

Overactivation of TRPV2 promotes ESCC growth and invasion in xenograft models

The biological role of TRPV2 in ESCC progression in vivo was investigated using BALB/c nude mice to generate a tumour xenograft model. In the ESCC formation assay, the tumours originating from Eca-109 cells followed recurrent brief heat (54 °C) challenge or O1821 (20 μM) application were significantly larger, in both size and weight, than the tumours from control cells, and these effects were attenuated markedly by tranilast (120 μM) (Fig. 4a–c). Notably, the tumours formed by TRPV2-knockout cells (Eca-109-$VR2^{-/-}$) followed recurrent brief heat (54 °C) treatment

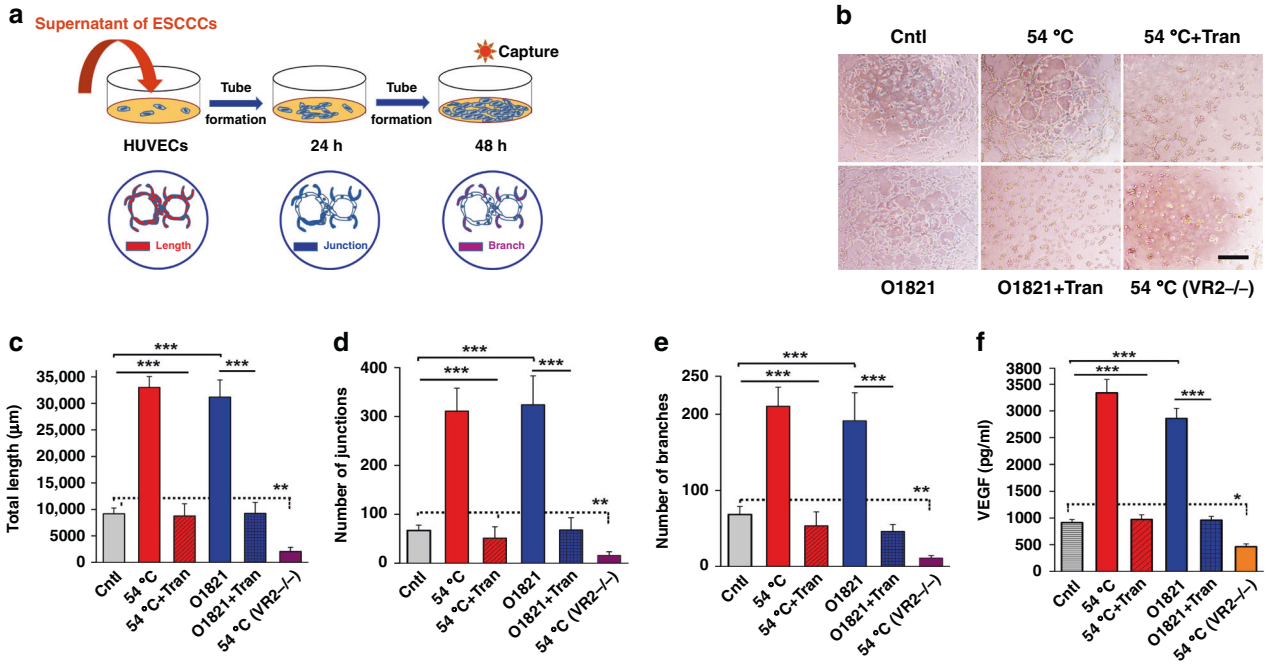

Fig. 3 Overactivation of TRPV2 in ESCC cells promotes tumour-associated angiogenesis. a Schematic diagram of the tube-formation assay. **b** Representative images of tube formation. The supernatant of cultured Eca-109 cells without specific treatment were used as controls. **c** The effect of overactivation of TRPV2 on the total length of the newly formed microvessels ($n = 3$). **d** The impact of overactivation of TRPV2 on the junction numbers of the newly formed microvessels ($n = 3$). **e** The effect of overactivation of TRPV2 on the branch numbers of the newly formed microvessels ($n = 3$). **f** The levels of VEGF were measured in the corresponding conditioned medium by ELISA ($n = 3$). HUVECs human umbilical vein endothelial cells, Cntl control, Tran tranilast, VR2$^{-/-}$: TRPV2 knocked-out Eca-109 cell line; Scale bar: 20 μm. *$P < 0.05$, **$P < 0.01$, ***$P < 0.001$ by two-way ANOVA tests.

were clearly smaller and had substantially lower tumour weights than the tumours formed by control cells (Fig. 4a–c). By contrast, wild-type NE2 cells were subcutaneously injected into the BALB/c nude mice, but no tumour formation was found even up to 30 days post inoculation. Conversely, when we used ectopically expressed TRPV2 NE2 (NE2-VR2) cells (Supplementary Fig. S6A, B) to perform the similar experiments, on day 12 after inoculation, tumours were palpable in the groups which were subcutaneously injected with NE2-VR2 cells followed recurrent brief heat (54 °C) challenge or O1821 (20 μM) application. At the end of the assay, it was observed that overactivation of TRPV2 by recurrent brief heat (54 °C) challenge or O1821 (20 μM) treatment could significantly promote tumour formation, which was displayed with larger tumour sizes and greater tumour weights compared to the control group, and these effects were compromised markedly by tranilast (120 μM) (Supplementary Fig. S6C–E). These findings further verified that overactivation of TRPV2 could significantly promote ESCC tumour formation in nude mouse models.

Moreover, an experimental tail vein metastasis model was established using BALB/c nude mice. The photon flux of Eca-109-gl cells (GFP and luciferase dual-labelled Eca-109 cells) followed recurrent acute heat (54 °C) challenge or O1821 (20 μM) administration to the lungs was profoundly enhanced compared with that in the control group, and these effects were attenuated significantly by tranilast (120 μM) application or by TRPV2 knockout using CRISPR–Cas9 (Fig. 4d and Supplementary Fig. S6F), suggesting that overactivation of TRPV2 markedly promotes the ability of Eca-109-gl cells to metastasise to the lungs following cell injection through the tail vein. Lungs derived from the group followed overactivation of TRPV2 in ESCC cells by recurrent acute heat (54 °C) challenge showed more metastatic tumour nodules than lungs from the control group (the rightmost panel of Fig. 4d). Consistently, the H&E staining of the lungs showed clear tumour lesions in the group followed by overactivation of TRPV2 in the ESCC cells by recurrent acute heat (54 °C) challenge, whereas tumour lesions were attenuated markedly by tranilast (120 μM). Meanwhile, tumour lesion was nearly absent from the TRPV2-knockout (Eca-109-gl-VR2$^{-/-}$) group (Fig. 4e). Immunohistocytochemical analysis revealed that the group followed overactivation of TRPV2 in ESCC cells by recurrent acute heat (54 °C) challenge showed markedly increased percentages of Ki-67-positive cells and of CD31-positive cells (which represents the proliferative cells and the newly formed microvessels respectively) compared to those of the control group (Fig. 4e–g). When combined with tranilast (120 μM), the group followed overactivation of TRPV2 in ESCC cells by recurrent acute heat (54 °C) challenge demonstrated much smaller Ki-67 proliferation indices and weaker newly formed microvessels signals (Fig. 4e–g), implying that overactivation of TRPV2 could promote tumour proliferation and tumour-related angiogenesis in vivo. Moreover, ESCC tumour formation under the skin, tumour metastasis to the lungs, the proliferation index and newly formed microvessels signal of the mouse lungs were all reduced by the knockout of TRPV2 (Fig. 4), further supported the notion that the driving role of TRPV2 in the progress of ESCC.

To sum up, these data suggest that the overactivation of TRPV2 contributes to the augmented proliferative, angiogenic and metastatic capacity of ESCC cells and hence drives ESCC progression in vivo.

Overactivation of TRPV2 activates HSP and PI3K/Akt/mTOR signalling pathways

To explore the mechanism(s) underlying the role that overactivation of TRPV2 plays in the progression of ESCC, the TRPV2-mediated signalling pathways had been screened and related key genes identified with an RNA-seq analysis under the condition of heat (54 °C) stimulation (cellular samples were sent to BGI company (Wuhan, China) to conduct the RNA-seq analysis). Pathways in cancer were found to be the most enriched and

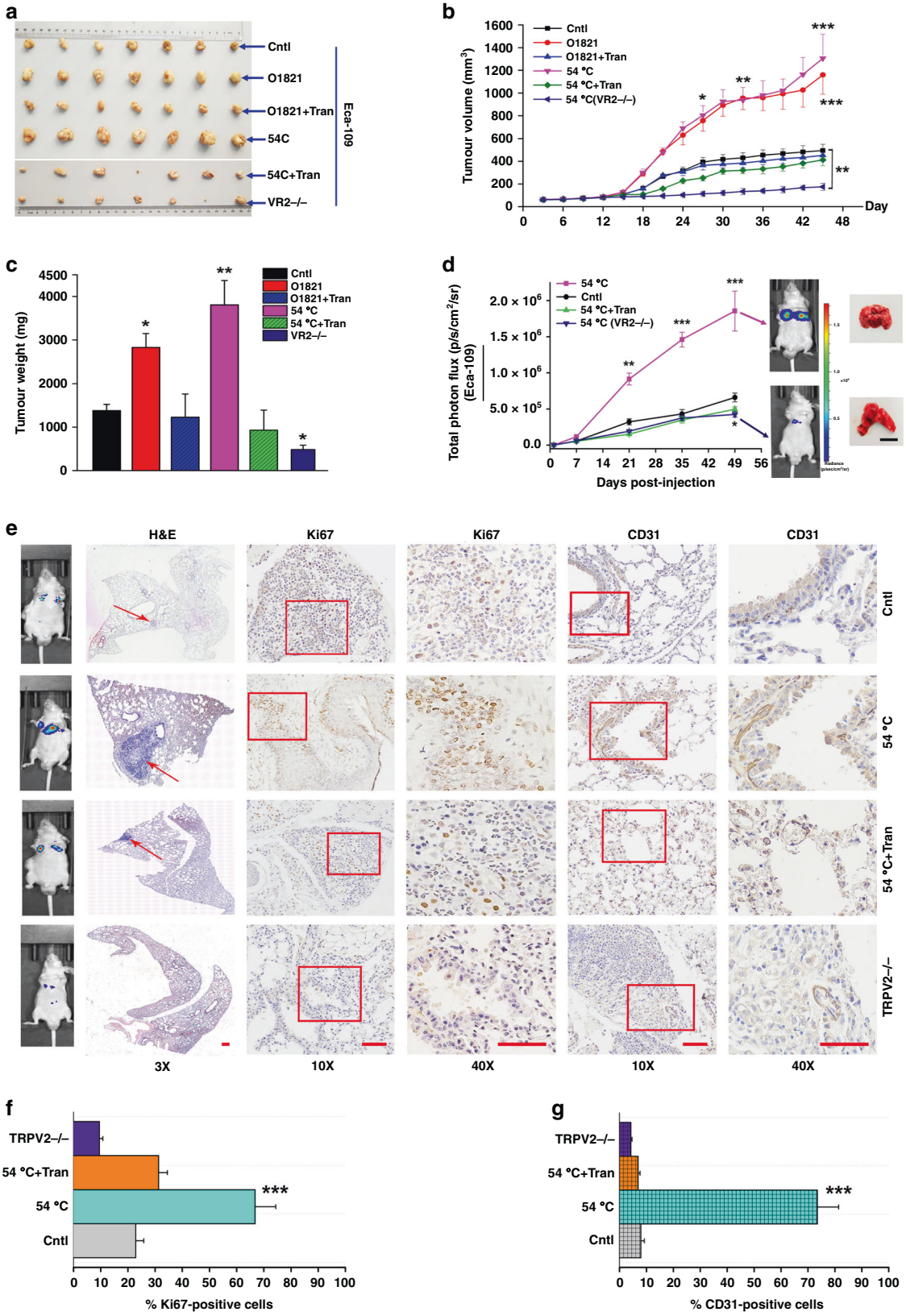

harboured the highest differentially expressed genes (DEGs) number in the signalling transduction in response to environmental cues under the condition of heat (54 °C) stimulation (Supplementary Fig. S7D–F). EIF4EBP and PI3K were revealed to be among the top upregulated DEGs under the condition of heat (54 °C) stimulation (Supplementary Fig. S8D). The results of the RNA-seq prompted us to detect pathways in response to heat stimulation (mainly the HSP pathway) and the PI3K pathway which

Fig. 4 Overactivation of TRPV2 promotes ESCC formation and invasion in nude mice. a Representative images of the tumours formed in mice in each group. Cultured Eca-109 cells without specific treatment were used as controls. **b** Tumour volumes were measured on the indicated days and plotted over time ($n = 2$). **c** Mean tumour weights were compared between different groups ($n = 2$). **d** Photon flux was measured on the indicated days and plotted over time. Representative images of tumour-bearing mice and lungs from mice in the control group and the group that followed heat (54 °C) stimuli in ESCC cells are shown on the right ($n = 2$). Cultured Eca-109-gl cells without specific treatment were used as controls. **e** H&E and IHC staining exhibited that overactivation of TRPV2 promoted the ESCC cells invasion into the lungs and promoted cellular proliferation and angiogenesis in the lungs, as indicated by percentages of Ki-67-positive cells (**f**) and CD31-positive cells (**g**), respectively, whereas pharmaceutical inhibition or knockout of TRPV2 reduced all these indices ($n = 5$). Cntl control; Tran tranilast; $TRPV2^{-/-}$ (or $VR2^{-/-}$) TRPV2 knocked-out Eca-109 cell line; Scale bar: 5 mm [in (**d**)]; 500 μm [in (**e**) ×3 and ×10]; 250 μm [in (**e**) ×40]. $^{*}P < 0.05$, $^{**}P < 0.01$, $^{***}P < 0.001$ by two-way ANOVA tests.

may play important role(s) in the TRPV2-mediated signalling cascades.

Firstly, the expression of HSF1, HSP70 and the PI3K pathway-activated genes were significantly upregulated at the transcriptional level following overactivation of TRPV2 upon exposure to heat stimuli (54 °C) or O1821 (20 μM), whereas the PI3K pathway negative regulator PTEN was downregulated under these conditions (Supplementary Fig. S9A, B), indicating that the HSP and PI3K pathway were activated while the TNFα and NFκB signal were not modulated by the overactivation of TRPV2 during these processes. Furthermore, western blot was carried out to verify the signalling cascade following the overactivation of TRPV2. Eca-109 cells were treated as described in "Drug administration and thermal stimulation protocol" (see "Methods") prior to western blotting assay.

In line with the findings of RT-qPCR, HSF1 was upregulated at the translational level by overactivation of TRPV2 by heat stimuli (54 °C) or the application of O1821 (20 μM), and this effect was inhibited by tranilast (120 μM) or TRPV2 knockout using CRISPR–Cas9 (Fig. 5e, f), indicating that HSF1 was modulated during the overactivation of TRPV2.

It is well known that HSF1 mediates heat shock stress within organisms; therefore, five members of the HSP family, including HSP27, HSP40, HSP60, HSP70 and HSP90, were examined during the assay, and only HSP70 and HSP27 were found to be upregulated by overactivation of TRPV2 upon exposure to heat stimuli (54 °C) or O1821 (20 μM) (Fig. 5a–c, e, f). The expression levels of both proteins were returned to near baseline when the activation was antagonised by tranilast (120 μM) or by TRPV2 knockout using CRISPR–Cas9, suggesting that the expression of these HSP proteins was mediated by TRPV2 (Fig. 5a, c, e, f). Previous works had reported that these two HSP proteins are involved in the progression of multiple types of cancers [40–42]. HSP70 and HSP27 may also play a role in the tumorigenesis of ESCC following the overactivation of TRPV2. The expression levels of calmodulin were inversely proportional to the overactivation of TRPV2 (Fig. 5b, d), possibly because more calmodulin protein was employed to modulate the increased influx of Ca^{2+} following overactivation of TRPV2, which is consistent with the results of Ca^{2+} imaging assays (Supplementary Fig. S2A, B, E, F).

Given that noxious heat stimulation may induce inflammatory reactions and based on the analysis of RNA-seq (Supplementary Fig. S8), we then measured two important inflammation-related pathways, PI3K and NFκB. The expression of PI3K was enhanced with the overactivation of TRPV2 by either heat stimuli (54 °C) or O1821 (20 μM), and these effects were inhibited by the TRPV2 inhibitor tranilast (120 μM) or by TRPV2 knockout using CRISPR–Cas9, whereas the level of NFκB proteins remained unchanged during the overactivation of TRPV2 (Fig. 5e, f), suggesting that PI3K may be involved in the overactivation of TRPV2, while NFκB is not, which is in accordance with the results of RT-qPCR (Supplementary Fig. S9).

To investigate the PI3K pathway playing in the progression of ESCC driven by the overactivation of TRPV2, we measured the expression of up- and downstream signalling proteins of this pathway. PDK1, which can be activated by PI3K, was found to be upregulated upon overactivation of TRPV2, and as expected, AKT1 and mTORC1, the target proteins of PDK1, were accordingly upregulated by overactivation of TRPV2 (Fig. 5g, h). In contrast, PTEN, the negative regulatory protein of PI3K, was conversely regulated during the process of overactivation of TRPV2 (Fig. 5g, h), which is consistent with the findings of RT-qPCR (Supplementary Fig. S9), suggesting that the PI3K signal was activated during the overactivation of TRPV2 and may be amplified by PTEN, thus significantly promoting the aggressiveness of ESCC upon overactivation of TRPV2.

In addition, it is worth noting that TNFα was upregulated by heat stimuli, while this effect may not be regulated by TRPV2 because its expression remained unchanged when tranilast (120 μM) was simultaneously applied or TRPV2 was knocked out using CRISPR–Cas9 (Fig. 5e, f and Supplementary Fig. S9). The activation of TNFα results in cell death [43]. Indeed, we did observe a small portion of cell death during the heat stimulation process, while the overall cell numbers were not decreased but increased in response to the overactivation of TRPV2 (Fig. 1d, f), suggesting that both pro-cell death and pro-cell proliferation signals could be simultaneously activated during the process of overactivation of TRPV2 by heat stimuli, while the latter signal exceeded the former, thus leading to the substantial increase in ESCC cell numbers upon overactivation of TRPV2.

To further explore the underlying mechanism of the role that overactivation of TRPV2 playing in the progress of ESCC, the phosphorylation levels of the signalling protein of PI3K pathway and its downstream molecular phosphorylation status were determined by western blot. Both phosphorylated Akt at S473 and T308 were significantly enhanced under the overactivation of TRPV2 mediated by either exposure to recurrent brief heat (54 °C) stimuli or the treatment of O1821 (20 μM) and these effects were inhibited by tranilast (120 μM) or the knockout of TRPV2 [p-Akt (T308)] (Supplementary Fig. S10A, B), indicating that the full activation of Akt was modulated by TRPV2. The levels of p-mTOR (S2448) paralleled to those of p-Akt (S473 and T308), suggesting its activation by Akt. p-p70S6K (T389) and p-4EBP1 (S65) were both substantially increased under the overactivation of TRPV2 mediated by either exposure to recurrent brief heat (54 °C) stimuli or the application of O1821 (20 μM) and these effects were inhibited by tranilast (120 μM), which are in agreement with the alteration of p-mTOR (S2448), suggesting both were activated by their upstream p-mTOR. The expression of the adapter protein Raptor was also found to be markedly upregulated under the overactivation of TRPV2 mediated by either exposure to recurrent brief heat (54 °C) stimuli or the treatment of O1821 (20 μM) and these effects were inhibited by tranilast (120 μM) or the knockout of TRPV2 (Supplementary Fig. S10A, B), which is consistent with the assembly of the mTORC1 complex during the signalling cascade. The sequential activation of PI3K, Akt, mTOR and their downstream substrates promotes protein synthesis, cell growth, cell survival and motility by activating their downstream kinases, including p70S6K and 4EBP1 [44]. Taken together, these findings corroborate that the activation of PI3K/Akt/mTOR involved in the TRPV2-mediated signalling transduction in driving the tumorigenesis of ESCC.

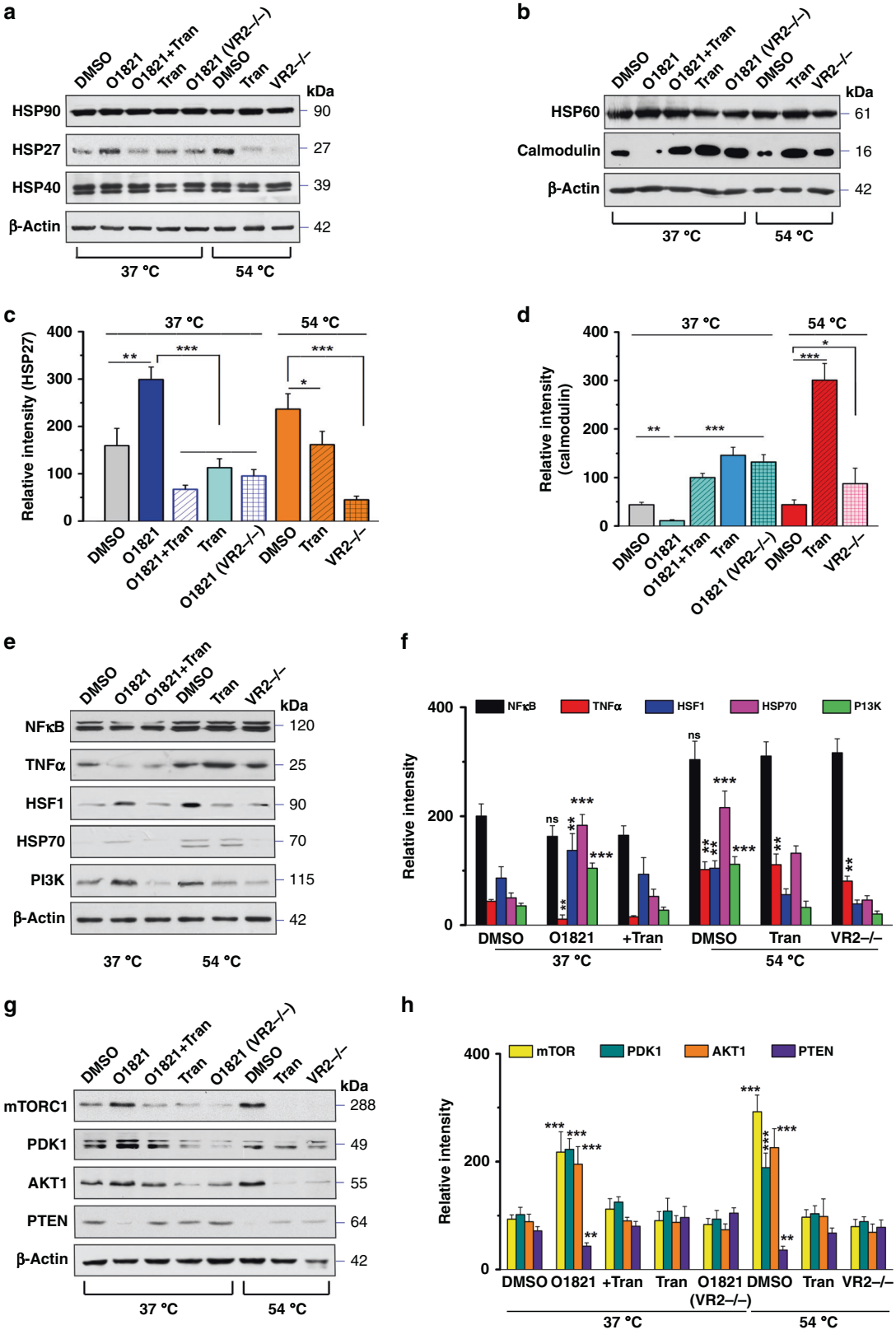

Last, to confirm the role of TRPV2-PI3K/Akt/mTOR playing in the progression of ESCC, VS5584 (a pan-PI3K/mTOR kinase inhibitor) and oroxin B (a PTEN protein activator and a pan-PI3K/mTOR kinase inhibitor) were applied in the Eca-109 cellular proliferation assay. As expected, both compounds could significantly attenuated Eca-109 proliferation following overactivation of TRPV2 by frequent acute heat (54 °C) challenge or O1821 application. The cellular proliferation of Eca-109 was further attenuated or abolished by the combination of VS5584 with oroxin B or by the co-administration with tranilast (Supplementary Fig. S11A, B).

Fig. 5 TRPV2 activation mediates HSP and PI3K signalling pathways. a Proteins levels of the HSP90, HSP40 and HSP27 were measured via western blotting. DMSO were used as experimental controls and β-actin was used as an internal control. **b** Protein levels of HSP60 and calmodulin were measured via western blotting. **c** Densitometric quantification of HSP27 protein, which was normalised relative to β-actin and compared ($n = 4$). **d** Densitometric quantification of calmodulin protein, which was normalised relative to β-actin and compared ($n = 4$). **e** Protein levels of HSF1, HSP70, NFκB, TNFα and PI3K were measured via western blotting. **f** Densitometric quantification of proteins in **e**, which were normalised relative to β-actin and compared ($n = 3$–5). **g** PI3K signalling pathway related proteins were measured via western blotting. **h** Densitometric quantification of proteins in **g**, which were normalised relative to β-actin and compared ($n = 3$–5). DMSO dimethyl sulfoxide, Tran tranilast, $VR2^{-/-}$ TRPV2 knocked-out Eca-109 cell line. $^{*}P < 0.05$, $^{**}P < 0.01$, $^{***}P < 0.001$ by two-way ANOVA tests.

Thus, we further verified the driving role of the TRPV2-PI3K/Akt/mTOR axis in the progression of ESCC. Taken together, these data suggest that the HSP and PI3K/Akt/mTOR signalling pathways participate in the overactivation of TRPV2 and may play an important role in the tumorigenesis of ESCC upon the overactivation of TRPV2 (Supplementary Fig. S11C). The combination of pan-PI3K/mTOR inhibitor and/or a PTEN activator with tranilast may be used for the prevention and treatment of ESCC.

TRPV2 is upregulated in ESCC tumour tissues

To ask the question of whether tumour tissues from patients have similar TRPV2 expression patterns to the ESCC cells used in the present study, we performed western blotting on 31 fresh samples derived from ESCC patients to detect the expression of TRPV2 protein and conducted IHC on 193 pathological slides of ESCC patients obtained from multiple hospitals (patient information is shown in Supplementary Table S2).

As expected, upregulation of TRPV2 was found in over 87% (27 out of 31 cases) of the fresh ESCC tissues compared with their matched adjacent non-tumour tissues (Fig. 6a–c). The staining of TRPV2 in the IHC assay showed that, in comparison to the non-tumour tissue, upregulation of TRPV2 was found in 84.1% of ESCC tumour tissues compared with adjacent non-tumour tissues (Fig. 6d, f, g). Intriguingly, the expression of TRPV2 was found to be upregulated among 77.5% of the squama of the para-tumour in the tumour slides compared with that of the non-tumour slides (Fig. 6e, g). We speculate that these TRPV2-positive cells in the squama of the para-tumour tissues may be invasive ESCC cells or untransformed squamous epithelial cells with highly expressed TRPV2 which prone to be activated by heat during food intake, while further efforts are needed to identify this aspect.

High expression level of TRPV2 was associated with poor survival in ESCC

The relationship between the expression of TRPV2 and prognosis of ESCC patients was investigated using data provided by authors of previous reports [28, 29]. Kaplan–Meier analysis demonstrated that patients with high level of TRPV2 expression had an unfavourable 5-year disease-specific survival (DSS) (62.4 vs 76.3%, $P < 0.05$) and disease-free survival (DFS) (55.8 vs 71.7%, $P < 0.05$) when compared to low expression (Fig. 7). The final multivariate survival analysis revealed that the strong expression of TPRV2 was an independent poor prognostic factor in patients with ESCC. These data corroborated that TRPV2 plays a crucial role in the progression of ESCC and suggest that TRPV2 has potential as a poor prognostic biomarker and novel therapeutic target for ESCC.

DISCUSSION

In this study, we found that a member of the temperature-sensitive transient receptor potential vanilloid receptor subfamily, i.e., TRPV2, was upregulated in esophageal squamous cell carcinoma (ESCC) cell lines and clinical ESCC samples compared with non-tumour control subjects. Further, the TRPV2 protein was found to be predominantly localised to the plasma membrane of the cells and was functionally active. Since TRPV2 is a noxious heat-activated ion channel validated by previous works, and exposure of the esophageal mucosa to heat stimuli has believed to be an important risk factor for the initiation and development of ESCC [14, 45, 46], we tested the impact of activation of TRPV2 by thermal stimuli (54 °C) and a chemical agonist (O1821, 20 μM) on the cancerous behaviours of ESCC cell lines including cellular proliferation, migration and invasion. We found that the overactivation of TRPV2 by recurrent brief thermal stimuli or O1821 application could significantly promote all these malignant behaviours, indicating that TRPV2 plays a role in the development of ESCC.

In this study, we developed a new method, i.e., single-cell culturing method, to evaluate cellular proliferation of ESCC cells. Although many hold that cancer may be originated from a very small portion of cancer stem cells (CSC) [47–49], during our experiments, we found that even a single ESCC cell could survive the extremely unfavourable culturing conditions and continues to be proliferative (they can survive an "old" medium which was not renewed for as long as 35 days, while non-tumour cells such as NE2 cells could not survive this condition for longer than 1 week). Therefore, it is feasible to examine cellular proliferation at a single-cell level and it will be more precise than conventional methods (such as methods using MTT and CCK8) on evaluation of the proliferation viability of cancer cells. Furthermore, it is comparable with the traditional CCK8 method. It would be more precise to investigate pro-tumorigenic factors, to test new chemicals on cancer cells or to predict therapeutic regimens using this single-cell culturing method. Nevertheless, more efforts are needed to prove its practicality on the culturing of other types of cancer cells. In addition, we applied a set of 3D-culturing chips devised by MIT researchers [50] to the cellular invasion assay. Three-dimensional culturing could better mimic in vivo cancer microenvironment and will be better in predicting the outcome of a cellular invasion assay [51–53]. Therefore, together with others, we propose that 3D culturing is a better option to assess the invasive ability of cancer cells [54, 55].

The pro-angiogenic process of cancer cells is believed to be an important step in tumour growth and development [39, 56]. Herein, we found that overactivation of TRPV2 could markedly promote angiogenesis in the tube-formation assay, thus further support that the pro-tumorigenic role of TRPV2 in the progression of ESCC may partly attribute to its pro-angiogenic potential.

When we translated the outcomes to an in vivo assay, we found that overactivation of TRPV2 could substantially promote both xenograft tumour formation under the skin through subcutaneous injection and tumour metastasis to the lungs via tail injection, the signals of the proliferative cells (Ki-67-positive) and newly formed microvessels (CD31-positive) were significantly upregulated, whereas pharmacological inhibition of TRPV2 and especially TRPV2 knockout using CRISPR–Cas9 showed clearly reduced tumour formation, metastasis and related indices in vivo, which is consistent with and further verified the pro-malignant behaviours observed during the in vitro experiments. It is worth noting that multiple malignant behaviours of the Eca-109 cells were sufficiently attenuated by the knockout of TRPV2 using CRISPR–Cas9 technique, it might imply, from the loss of function's (LOF) perspective, that TRPV2 may be oncogenic per se.

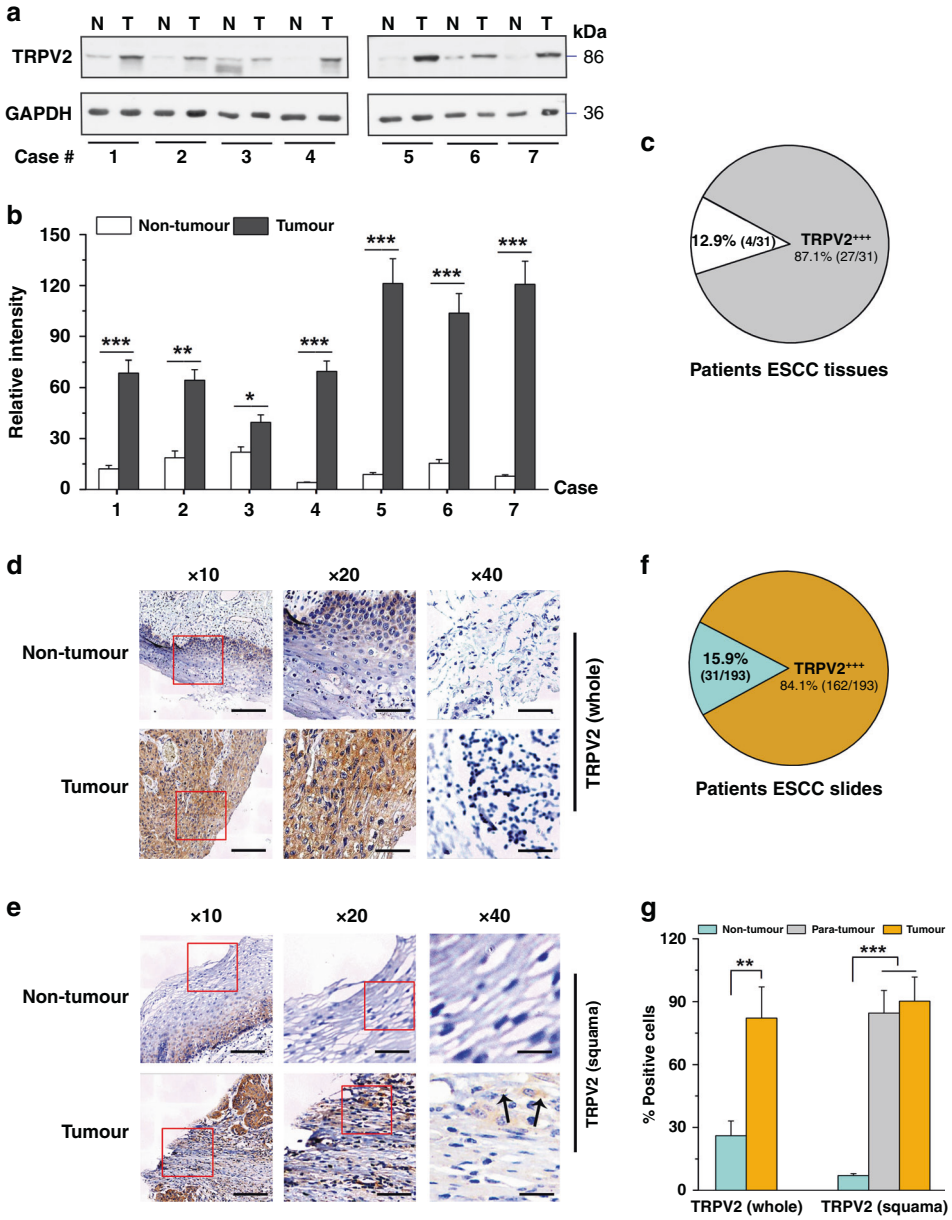

Fig. 6 TRPV2 expression profile in ESCC patients. a Samples from ESCC and adjacent non-tumour tissues which were obtained during surgical procedures were subjected to western blotting to measure the expression of TRPV2. GAPDH was used as an internal control. Seven ESCC cases are shown here. **b** Densitometric quantification of TRPV2 protein among ESCC and adjacent non-tumour tissues ($n = 3$). **c** Percentage of TRPV2 upregulation ($TRPV^{+++}$) among ESCC patients (fresh tumour samples) are shown. **d** Immunohistochemistry of slides of ESCC and adjacent non-tumour tissues from ESCC patients to detect the expression profile of TRPV2. Selected fields of the slides are magnified at ×20 and are shown. The rightmost microphotographs are derived from a negative control group (×40). **e** Immunohistochemistry of slides of ESCC and adjacent non-tumour tissues from ESCC patients to detect the expression profile of TRPV2. The fields of the squama in both para-tumour area of the ESCC slides and adjacent non-tumour slides were magnified at ×20 and further at ×40 and are shown. **f** Percentage of TRPV2 upregulation ($TRPV^{+++}$) among ESCC patients (paraffin tumour slides) are shown. **g** Summary of TRPV2-positive cells in **d**, **e** ($n = 193$). Scale bar: 50 μm at ×10, 25 μm at ×20 and 12.5 μm at ×40. $^{*}P < 0.05$, $^{**}P < 0.01$, $^{***}P < 0.001$ by paired Student's *t* test or one-way ANOVA tests.

Conversely, the wild-type non-tumour cell line NE2 did not show any of these properties; however, when TRPV2 was overexpressed by transfection of the TRPV2 plasmid into the wild-type cells (to establish NE2-VR2 cells), we found that the overactivation of TRPV2 in NE2-VR2 cells could promote markedly cellular proliferation, migration and invasion of the cells. Tumour formation also was observed by subcutaneously injecting these cells into the BALB/c nude mice. This cell property switch further corroborates that TRPV2 may play an important role in the initiation and development of ESCC.

In organisms or the cells, thermal stress may exert effects on multiple signalling pathways [57–59], based on previous reports [60–62] and the data of the RNA-seq, we focused on the TRPV2-related pathways. We found that at least 3 pathways were activated during the overactivation of TRPV2, including HSPs (HSP70, HSP27), TNFα and PI3K pathways. Overactivation of TRPV2 could activate the signal of PI3K and its downstream signals (PDK1, mTOR and Akt1) at both mRNA and protein levels, while its negative regulator (PTEN) was simultaneously inhibited; thus, the PI3K signals were amplified. Furthermore, we found that the full

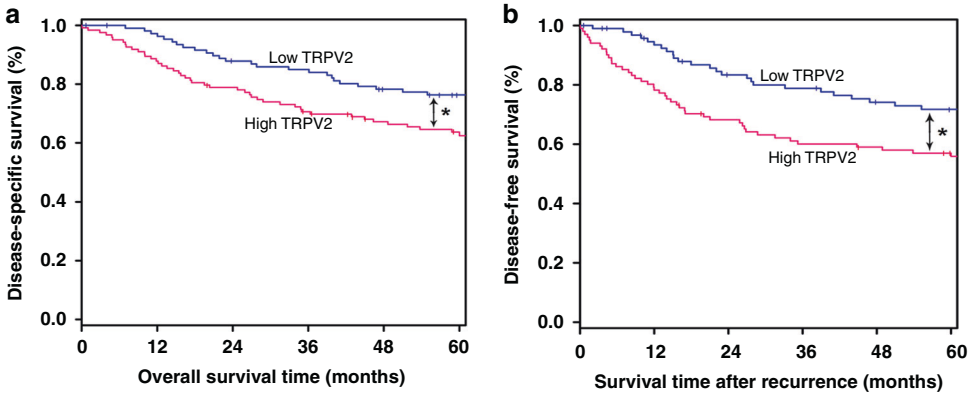

Fig. 7 High expression level of TRPV2 was associated with worse survival in ESCC. a Survival curves showed that patients with high expression of TRPV2 had a poorer disease-specific survival than those with low expression, the low group ($n = 109$) and the high group ($n = 123$). **b** Patients with high expression of TRPV2 had a worse disease-free survival than those with low expression, the low group ($n = 95$) and the high group ($n = 101$). *$P < 0.05$ by log-rank test.

activation of Akt (phosphorylation at S473 and T308) was modulated by TRPV2. The phosphorylation of downstream signalling proteins [p-mTOR (S2448), p-p70S6K (T389) and p-4EBP1 (S65)] were all upregulated by the overactivation of TRPV2 mediated by either exposure to recurrent brief heat (54 °C) stimuli or the application of O1821 (20 μM) The sequential activation of PI3K, Akt, mTOR and their downstream substrates promotes protein synthesis, cell growth, cell survival and motility by activating their downstream kinases, including p70S6K and 4EBP1, thus promoted the progress of tumorigenesis in ESCC. Taken together, these findings verified that the activation of PI3K/Akt/mTOR involved in the TRPV2-mediated signalling transduction.

The PI3k pathways have been found to be involved in the progression of numerous cancer forms [63–65]. Two small molecular compounds, VS5584 (a pan-PI3K/mTOR kinase inhibitor) and oroxin B (a PI3K/mTOR inhibitor and PTEN activator), were used in the cellular proliferation assay to further verify these findings. As expected, both compounds could abolish the cellular proliferation of ESCC cells following overactivation of TRPV2 in the cells, which suggests that TRPV2-PI3K/mTOR may be used as a novel target for the prevention and treatment of ESCC.

We also assessed more than 200 ESCC patient samples, including fresh samples and paraffin slides, and found that TRPV2 was upregulated among >87% of the fresh tumour samples and >84% of the tumour slides compared with the non-tumour control samples. Specifically, the expression of TRPV2 was found to be upregulated among >70% of the squama of the para-tumour in the tumour slides compared with that of the non-tumour slides. We speculate that those TRPV2 positive may either be invasive ESCC cells or untransformed squamous epithelial cells with highly expressed TRPV2 which are prone to be thermally activated during food intake. While further investigation is warranted.

Previously, Atsushi et al. [66] proposed that TRPV2 is involved in the maintenance of CSCs (cancer stem cells) of ESCC. Analysis using data provided by previous studies [28, 29] revealed that patients with the high level of TRPV2 expression had a worse 5-year disease-specific survival and disease-free survival compared to low expression. And the strong expression of TPRV2 was an independent poor prognostic factor in patients with ESCC. These findings mutually confirmed with ours regarding the role of TRPV2 in driving the progression of ESCC. We further uncover a mechanism underlying the heat-challenging-related pathogenesis of ESCC and provide molecular insights into the correlation of heat exposure on the esophageal mucosa with ESCC initiation and development which could be used as a novel target for the prevention and treatment of ESCC.

Although great advances have been made in the detection and treatment of ESCC in the past decade, the outcomes of many patients still remain grim [67–69]; better preventive methods and therapeutic strategies are urgently needed for a better clinical prospect of ESCC patients. Surprisingly, our findings suggest that the temperature (54 °C) of thermal stimuli activating TRPV2 channel and driving the progress of ESCC is much lower than the dietary temperatures among many populations [21–23], therefore, to advise the communities to stay away from high-temperature food could be an option.

To summarise, in this study, we found that the transient receptor potential vanilloid receptor 2 (TRPV2) was upregulated in ESCC cell lines and in ESCC tumour samples compared with non-tumour control subjects. Overactivation of TRPV2 promotes ESCC cancerous behaviours in vitro and enhances the tumorigenesis of ESCC in vivo. The pro-tumorigenic role of TRPV2 was found to occur mainly via the mediation of the HSP70/27 and PI3K/Akt/mTOR signalling pathways. Our current study, for the first time, reveals an important mechanism underlying the progression of ESCC upon thermal stress and uncovers the TRPV2-PI3K/Akt/mTOR pathway as a promising target for the prevention and treatment of ESCC. On the basis of our findings and the applicability of tranilast in the clinic, a cooperative investigation has been initiated, aiming at translating this drug into clinical ESCC trials.

DATA AVAILABILITY

The data in this study are available from the corresponding author upon reasonable request.

REFERENCES

1. Florea A, Sangaré L, Lowe K. A multinational assessment of gastric, esophageal, and colorectal cancer burden: a report of disease incidence, prevalence, and fatality. J Gastrointest Cancer. 2020;51:965–71.
2. Ferlay J, Shin HR, Bray F, Forman D, Mathers C, Parkin DM. Estimates of worldwide burden of cancer in 2008: GLOBOCAN 2008. Int J Cancer. 2010;127:2893–917.
3. Ma G, Zhang J, Jiang H, Zhang N, Zhu Y, Deng Y, et al. Microvessel density as a prognostic factor in esophageal squamous cell cancer patients: a meta-analysis. Medicine. 2017;96:e7600.
4. Domper Arnal MJ, Ferrández Arenas Á, Lanas Arbeloa Á. Esophageal cancer: risk factors, screening and endoscopic treatment in Western and Eastern countries. World J Gastroenterol. 2015;21:7933–43.
5. Castellsagu´e X, Munoz N, Stefani E. Influence of mate drinking, hot beverages and diet on esophageal cancer risk in south America. Int J Cancer. 2000;88:658–64.
6. Song Q, Jiang D, Wang H, Huang J, Liu Y, Xu C, et al. Chromosomal and genomic variations in esophageal squamous cell carcinoma: a review of technologies, applications, and prospections. J Cancer. 2017;8:2492–2500.

7. McCormack VA, Menya D, Munishi MO, Dzamalala C, Gasmelseed N, Leon Roux M, et al. Informing etiologic research priorities for squamous cell esophageal cancer in Africa: a review of setting-specific exposures to known and putative risk factors. Int J Cancer. 2017;140:259–71.
8. Islami F, Boffetta P, Ren JS, Pedoeim L, Khatib D, Kamangar F. High-temperature beverages and foods and esophageal cancer risk-a systematic review. Int J Cancer. 2009;125:491–524.
9. Siegel R, Naishadham D, Jemal A. Cancer statistics. CA Cancer J Clin. 2012;62:10–29.
10. Enzinger PC, Mayer RJ. Esophageal cancer. N. Engl J Med. 2003;349:2241–52.
11. Abnet CC, Arnold M, Wei WQ. Epidemiology of esophageal squamous cell carcinoma. Gastroenterology. 2018;154:360–73.
12. Lin S, Xu G, Chen Z, Liu X, Li J, Ma L, et al. Tea drinking and the risk of esophageal cancer: focus on tea type and drinking temperature. Eur J Cancer Prev. 2020; e-pub ahead of print; https://doi.org/10.1097/CEJ.0000000000000568.
13. Gao Y, Hu N, Han XY, Ding T, Giffen C, Goldstein AM, et al. Risk factors for esophageal and gastric cancers in Shanxi Province, China: a case-control study. Cancer Epidemiol. 2011;35:e91–99.
14. Tai WP, Nie GJ, Chen MJ, Yaz TY, Guli A, Wuxur A, et al. Hot food and beverage consumption and the risk of esophageal squamouscell carcinoma: a case-control study in a northwest area in China. Medicine. 2017;96:e9325.
15. Loomis D, Guyton KZ, Grosse Y, Lauby-Secretan B, El Ghissassi F, Bouvard V, et al. International Agency for Research on Cancer Monograph Working Group, carcinogenicity of drinking coffee, mate, and very hot beverages. Lancet Oncol. 2016;17:877–8.
16. Okaru AO, Rullmann A, Farah A, Gonzalez de Mejia E, Stern MC, Lachenmeier DW. Comparative esophageal cancer risk assessment of hot beverage consumption (coffee, mate and tea): the margin of exposure of PAH vs very hot temperatures. BMC Cancer. 2018;18:236–46.
17. Monet M, Lehenkyi V, Gackiere F, Firlej V, Vandenberghe M, Roudbaraki M, et al. Role of cationic channel TRPV2 in promoting prostate cancer migration and progression to androgen resistance. Cancer Res. 2010;70:1225–1235.
18. Elbaz M, Ahirwar D. TRPV2 is a novel biomarker and therapeutic target in triple negative breast cancer. Oncotarget. 2016;5:27–39.
19. Clapham DE, Montell C, Schultz G, Julius D. International Union of Pharmacology International Union of Pharmacology XLIII Compendium of voltage-gated ion channels: transient receptor potential channels. Pharm Rev. 2003;55:591–6.
20. Liu G, Xie C, Sun F, Xu X, Yang Y, Zhang T, et al. Clinical significance of transient receptor potential vanilloid 2 expression in human hepatocellular carcinoma. Cancer Genet Cytogenet. 2010;197:54–59.
21. Islami F, Pourshams A, Nasrollahzadeh D, Kamangar F, Fahimi S, Shakeri R, et al. Tea drinking habits, esophageal cancer in a high risk area in northern Iran: population based case–control study. BMJ. 2009;338:b929.
22. Michael OM, Rachel H, Oscar M, Theonest N, Arnold N, Joachim S, et al. Africa's esophageal cancer corridor: do hot beverages contribute? Cancer Causes Control. 2015;26:1477–86.
23. Islami F, Boffetta P, Ren JS, Pedoeim L, Khatib D, Kamangar F. High-temperature beverages and foods and esophageal cancer risk—a systematic review. Int J Cancer. 2009;125:491–524.
24. Huang R, Wang F, Yang Y, Ma W, Lin Z, Cheng N, et al. Recurrent activations of transient receptor potential vanilloid-1 and vanilloid-4 promote cellular proliferation and migration in esophageal squamous cell carcinoma cells. FEBS Openbio. 2019;9:206–25.
25. Ma W, Li C, Yin S, Liu J, Gao C, Lin Z, et al. Novel role of TRPV2 in promoting the cytotoxicity of H2O2-mediated oxidative stress in human hepatoma cells. Free Radic BiolMed. 2015;89:1003–13.
26. Xie J, Ge W, Li N, Liu Q, Chen F, Yang X, et al. Efficient base editing for multiple genes and loci in pigs using base editors. Nat Commun. 2019;10:2852–65.
27. Bae S, Park J, Kim JS. Cas-OFFinder: a fast and versatile algorithm that searches for potential off-target sites of Cas9 RNA-guided endonucleases. Bioinformatics. 2014;30:1473–5.
28. Zhou K, Zhang SS, Yan Y, Zhao S. Overexpression of transient receptor potential vanilloid 2 is associated with poor prognosis in patients with esophageal squamous cell carcinoma. Med Oncol. 2014;31:17.
29. Michihiro K, Atsushi S, Yuzo Y, Keita K, Toshiyuki K, Katsutoshi S, et al. The expression and role of TRPV2 in esophageal squamous cell carcinoma. Sci Rep. 2019;9:16055.
30. Nilius B, Owsianik G, Voets T, Peters JA. Transient receptor potential cation channels in disease. Physiol Rev. 2007;87:165–217.
31. West AV, Wullkopf L, Christensen A, Leijnse N, Tarp JM, Mathiesen J, et al. Dynamics of cancerous tissue correlates with invasiveness. Sci Rep. 2017;7:43800–13.
32. Chiorazzi N, Ferrarini M. Cellular origin(s) of chronic lymphocytic leukemia: cautionary notes and additional considerations and possibilities. Blood. 2011;117:1781–91.
33. Teresina L, Cheng K, Tanner MR, He M, Beeton C, Yousef A-A, et al. The cation channel trpv2 is a new suppressor of arthritis severity, joint damage and synovial fibroblast invasion. Clin Immunol. 2015;158:183–92.
34. Offertaler L, Mo F-M, Biatkai S. Selective ligands and cellular effectors of a G protein-coupled endothelial cannabinoid receptor. Mol Pharmacol. 2003;63: 699–705.
35. Shin Y, Kim H, Han S, Won J, Jeong HE, Lee ES, et al. Hydrogels: extracellular matrix heterogeneity regulates three-dimensional morphologies of breast adenocarcinoma cell invasion. advanced healthcare. Materials. 2013;2:920–920.
36. Huang YL, Segall JE, Wu M. Microfluidic modeling of the biophysical microenvironment in tumor cell invasion. Lab Chip. 2017;17:3221–33.
37. Maciaczyk D, Picard D, Zhao L, Koch K, Herrera-Rios D, Li G, et al. CBF1 is clinically prognostic and serves as a target to block cellular invasion and chemoresistance of EMT-like glioblastoma cells. Br J Cancer. 2017;117:102–12.
38. Caporali S, Amaro A, Levati L, Alvino E, Lacal PM, Mastroeni S, et al. miR-126-3p down regulation contributes to dabrafenib acquired resistance in melanoma by up-regulating ADAM9 and VEGF-A. J Exp Clin Cancer Res. 2019;38:272–88.
39. Hanahan D, Weinberg RA. Hallmarks of cancer: the next generation. Cell. 2011;144:646–74.
40. Brünnert D, Langer C, Zimmermann L, Bargou RC, Burchardt M, Chatterjee M, et al. The heat shock protein 70 inhibitor VER155008 suppresses the expression of HSP27, HOP and HSP90β and the androgen receptor, induces apoptosis, and attenuates prostate cancer cell growth. J Cell Biochem. 2020;121:407–17.
41. Jin HO, Hong SE, Kim JY, Kim MR, Chang YH, Hong YJ, et al. Induction of HSP27 and HSP70 by constitutive overexpression of Redd1 confers resistance of lung cancer cells to ionizing radiation. Oncol Rep. 2019;41:3119–26.
42. Söderström HK, Kauppi JT, Oksala N, Paavonen T, Krogerus L, Räsänen J, et al. Overexpression of HSP27 and HSP70 is associated with decreased survival among patients with esophageal adenocarcinoma. World J Clin Cases. 2019;7:260–9.
43. Shen J, Xiao Z, Zhao Q, Li M, Wu X, Zhang L, et al. Anti-cancer therapy with TNFα and IFNγ: A comprehensive review. Cell Prolif. 2018;51:12441.
44. Feng Y, Chenl X, Cassady K, Zou Z, Yang S, Wang Z, et al. The role of mTOR inhibitors in hematologic disease: from bench to bedside. Front Oncol. 2021;10:10–25.
45. Mickle AD, Shepherd AJ, Mohapatra DP. Sensory TRP channels: the key transducers of nociception and pain. Prog Mol Biol Transl Sci. 2015;131:73–118.
46. Benham CD, Gunthorpe MJ, Davis JB. TRPV channels as temperature sensors. Cell Calcium. 2003;33:479–87.
47. Dawood S, Austin L, Cristofanilli M. Cancer stem cells: implications for cancer therapy. Oncology. 2014;28:1101–7.
48. Toh TB, Lim JJ, Chow EK. Epigenetics in cancer stem cells. Mol Cancer. 2017;16:29.
49. Nassar D, Blanpain C. Cancer stem cells: basic concepts and therapeutic implications. Annu Rev Pathol. 2016;23:47–76.
50. Boussommier-Calleja A, Li R, Chen MB, Wong SC, Kamm RD. Microfluidics: a new tool for modeling cancer-immune interactions. Trends Cancer. 2016;2:6–19.
51. Chaicharoenaudomrung N, Kunhorm P, Noisa P. Three-dimensional cell culture systems as an in vitro platform for cancer and stem cell modeling. World J Stem Cells. 2019;11:1065–83.
52. Song HH, Park KM, Gerecht S. Hydrogels to model 3D in vitro microenvironment of tumor vascularization. Adv Drug Deliv Rev. 2014;79:19–29.
53. Levinger I, Ventura Y, Vago R. Life is three dimensional-as in vitro cancer cultures should be. Adv Cancer Res. 2014;121:383–414.
54. Shen CN, Goh KS, Huang CR, Chiang TC, Lee CY, Jeng YM, et al. Lymphatic vessel remodeling and invasion in pancreatic cancer progression. EBioMedicine. 2019;47:98–113.
55. Iwai S, Kishimoto S, Amano Y, Nishiguchi A, Matsusaki M, Takeshita A, et al. Three-dimensional cultured tissue constructs that imitate human living tissue organization for analysis of tumor cell invasion. J Biomed Mater Res A. 2019;107:292–300.
56. Harper SJ, Bates DO. VEGF-A splicing: the key to anti-angiogenic therapeutics. Nat Rev Cancer. 2008;8:880–7.
57. Abdelnour SA, Abd El-Hack ME, Khafaga AF, Arif M, Taha AE, Noreldin AE. Stress biomarkers and proteomics alteration to thermal stress in ruminants: a review. J Therm Biol. 2019;79:120–34.
58. Somero GN. The cellular stress response and temperature: function, regulation, and evolution. J Exp Zool A Ecol Integr Physiol. 2020;333:379–97.
59. Burtscher M, Gatterer H, Burtscher J, Mairbäurl H. Extreme terrestrial environments: life in thermal stress and hypoxia—a narrative review. Front Physiol. 2018;9:572.
60. Chan CJ, Whyte G, Boyde L, Salbreux G, Guck J. Impact of heating on passive and active biomechanics of suspended cells. Interface Focus. 2014;4:20130069–80.
61. Yao J, Liu B, Qin F. Rapid temperature jump by infrared diode laser irradiation for patch-clamp studies. Biophysical J. 2009;96:3611–9.
62. Yao J, Liu B, Qin F. Modular thermal sensors in temperature-gated transient receptor potential (TRP) channels. Proc Natl Acad Sci USA. 2011;108:11109–14.

63. Su T, Huang L, Zhang N, Peng S, Li X, Wei G, et al. FGF14 functions as a tumor suppressor through inhibiting PI3K/AKT/mTOR pathway in colorectal cancer. J Cancer 2020;11:819–25.
64. Wang JX, Jia XJ, Liu Y, Dong JH, Ren XM, Xu O, et al. Silencing of miR-17-5p suppresses cell proliferation and promotes cell apoptosis by directly targeting PIK3R1 in laryngeal squamous cell carcinoma. Cancer Cell Int. 2020;20:14.
65. Vasan N, Toska E, Scaltriti M. Overview of the relevance of PI3K pathway in HR-positive breast cancer. Ann Oncol. 2019;30(suppl 10):x3–x11.
66. Shiozaki A, Kudou M, Ichikawa D, Fujiwara H, Shimizu H, Ishimoto T, et al. Esophageal cancer stem cells are suppressed by tranilast, a TRPV2 channel inhibitor. J Gastroenterol. 2018;53:197–207.
67. Lu YF, Yu JR, Yang Z, Zhu GX, Gao P, Wang H, et al. Promoter hypomethylation mediated upregulation of MicroRNA-10b-3p targets FOXO3 to promote the progression of esophageal squamous cell carcinoma (ESCC). J Exp Clin Cancer Res. 2018;37:301.
68. Hong Y, Ding ZY. PD-1 inhibitors in the advanced esophageal cancer. Front Pharmacol. 2019;10:1418.
69. Hirano H, Kato K. Systemic treatment of advanced esophageal squamous cell carcinoma: chemotherapy, molecular-targeting therapy and immunotherapy. Jpn J Clin Oncol. 2019;49:412–20.

ACKNOWLEDGEMENTS

We are grateful to Prof. GSW Tsao (Hong Kong University) for giving us the immortalised esophageal squamous cell line NE2 as a gift. We thank colleagues in GIBH, including Prof. Peng Li, Dr. Zhiwu Jiang for assistance in the establishment of GL-labelled cell lines, Dr. Kepin Wang, Dr. Jingke Xie for technical help with CRISPR–Cas9 editing and Prof. Liangxue Lai for giving us the Cas9-G418 plasmid. We thank prof. Huayu Qi for important comments on the manuscript.

AUTHOR CONTRIBUTIONS

Conception and design: Z Li and RH; development of methodology: RH, PZ, HZ and JX; acquisition of the data (provided animals, acquired and managed patients, provided facilities, etc.): PZ, WX, JX, Z Lin, and NC; analysis and interpretation of data (e.g., statistical analysis, biostatistics, computational analysis): RH, SL, CT, LW and YY; writing, review, and/or revision of the manuscript: RH, JdDH and Z Li; study supervision: Z Li; all authors reviewed and approved the final version of the manuscript.

FUNDING

This work was supported by Frontier Research Programs of Guangzhou Regenerative Medicine and Health Guangdong Laboratory (Grant Nos. 2018GZR110105020 and 2018GZR110105019), the National Natural Science Foundation of China (31671211) and the Science and Technology Planning Project of Guangdong Province, China (2017B030314056).

ETHICS APPROVAL AND CONSENT TO PARTICIPATE

All of the animal studies were conducted under protocols approved by the guidelines of the Ethics Committee of Animal Experiments at GIBH (No. 2016015). For the use of clinical materials for this study, prior patient consent and approval from the Institutional Research Ethics Committee of the Cancer Hospital of Hunan Province (No. CHH-YJ-0317005) and the Second Affiliated Hospital of Xiangya Medical School of Central South University (No. XY-2-18179) were obtained.

CONSENT TO PUBLISH

Not applicable.

COMPETING INTERESTS

The authors declare no competing interests.

ADDITIONAL INFORMATION

Supplementary information The online version contains supplementary material available at https://doi.org/10.1038/s41416-022-01896-2.

Correspondence and requests for materials should be addressed to Zhiyuan Li.

Reprints and permission information is available at http://www.nature.com/reprints

Publisher's note Springer Nature remains neutral with regard to jurisdictional claims in published maps and institutional affiliations.